Computer Networks 172 (2020) 107154

Contents lists available at ScienceDirect

Computer Networks

journal homepage: www.elsevier.com/locate/comnet

An analytical model for IEEE 802.11 with non-IEEE 802.11 interfering source

Patrick Bosch*, Steven Latré, Chris Blondia

University of Antwerp - imec, IDLab - Department of Mathematics and Computer Science, Sint-Pietersvliet 7, 2000 Antwerp, Belgium

ARTICLE INFO

2010 MSC:
68R01

Keywords:
IEEE 802.11
Wireless networks
Analytical model
Interference

ABSTRACT

The MAC layer of the IEEE 802.11 standard deploys a CSMA/CA protocol to regulate the access to the shared medium. Not only other IEEE 802.11 stations but also non-IEEE 802.11 devices can be a source of interference, causing collisions and, therefore, re-transmissions, leading to an increased packet latency and a decrease of throughput. As in general, the non-IEEE 802.11 devices do not employ the IEEE8 802.11 CSMA/CA protocol (in particular carrier sensing and the behavior when the medium is sensed busy), the impact of the interference they cause may lead to vital performance degradation of the IEEE 802.11 network. This impact of non-IEEE 802.11 interfering sources on the network performance has not been accurately modeled yet in literature. In this paper, we first characterize a non-IEEE 802.11 interfering source by employing an on-off process. Then we propose, based on earlier results from Bianchi, an analytical model to predict latency and throughput in a saturated as well as an unsaturated network, considering that an interfering source is present. The model utilizes a Markov chain to correctly characterize the behavior of the back-off algorithm of a tagged station in the presence of an interfering source, as well as a Quasi Birth-Death (QBD) process to model the station's packet queue behavior. We show that we can accurately estimate the impact of non-IEEE 802.11 inference on IEEE 802.11 performance. The model is validated through a comparison with measurements in a real IEEE 802.11 network as well as with an ns3-simulation, whereby a very good agreement is achieved (a difference less than 2%).

1. Introduction

Wireless networks, especially IEEE 802.11, are ubiquitous in today's world. The use cases range from small home networks to large-scale events like conferences and festivals [2,3]. In all cases, interference and collisions decline the performance significantly with an increasing number of stations and density. However, the origin of interference is not limited to other IEEE 802.11 stations. Non-IEEE 802.11 sources, such as other wireless network technologies, microwaves, screens, or Radio Frequency (RF) equipment, generate interference as well, especially if they are not well shielded. One such example is Long-Term Evolution (LTE) in the unlicensed band. In the presence of LTE, IEEE 802.11 can lose up to 98% of its throughput, while LTE barely loses any capacity at all [4]. This performance impact can be partially mitigated by communication between both systems or using duty cycling to silence sub-frames; although additional fine-tuning the parameters improves performance, it is complex [5–7].

IEEE 802.11 networks employ a Listen-Before-Talk (LBT) protocol to manage transmissions, implemented using a Carrier Sense Multiple Access with Collision Avoidance (CSMA/CA) protocol: before a station sends a packet, it senses the medium and only if the medium is idle, it will transmit the packet. Contrary, managed networks use a centralized resource allocation mechanism, such as LTE with scheduling. Carrier Sense (CS) and Energy Detection (ED) both sense the medium. The first detects and decodes IEEE 802.11 traffic and estimates how long the channel will be busy by reading the preamble of the packet. The latter detects energy that is above a threshold, specified by the hardware vendor. When a non-IEEE 802.11 interference source emits energy, the ED will detect its presence preventing IEEE 802.11 stations from sending if the detected energy is above a certain threshold. If it tries to send and a collision occurs because the interfering source becomes active during the transmission or another station tried to send as well, the station backs off with the value of the back-off timer randomly chosen from its current Contention Window (CW). The size of the CW doubles at each collision until it reaches the maximum size. If it reaches the maximum number of retries, the packet is dropped. Collisions with packets of other IEEE 802.11 sources always lead to packet loss. However, collisions with non-IEEE 802.11 sources can happen unnoticed, thanks to the Forward Error Correction (FEC) mechanism that can easily recover from the collision, in particular when a conservative data rate is used.

Interference from IEEE 802.11 stations already results in higher latency and lower throughput due to the employed back-off

* Corresponding author.
E-mail addresses: patrick.bosch@uantwerpen.be (P. Bosch), steven.latre@uantwerpen.be (S. Latré), chris.blondia@uantwerpen.be (C. Blondia).

https://doi.org/10.1016/j.comnet.2020.107154
Received 9 September 2019; Received in revised form 16 January 2020; Accepted 17 February 2020
Available online 19 February 2020

mechanism and the shared medium. With additional interference from non-IEEE 802.11 devices, the effect on performance multiplies. Non-IEEE 802.11 devices do not necessarily apply the LBT and CSMA/CA rules of the IEEE 802.11 Medium Access Control (MAC) protocol [8]. This effect is especially pronounced if the device does not follow any communication protocol, but generates energy that is detectable by IEEE 802.11 devices. Examples of such devices are not well-shielded screens or microwaves. A network with hidden terminals has similar problems as with a non-IEEE 802.11 source, but it can differ from an external source insofar as it still follows a communication protocol. The use of a communication protocol gives each node the possibility to successfully transmit as they back off after a collision, which leaves an open window for transmission. This behavior is completely different with a source that does not follow a communication protocol as it can become active at any point in time and does not necessarily leave a window for transmission.

These type of external sources that do not follow a communication protocol are present as every electrical device can act as such a source. Therefore, when evaluating the performance of IEEE 802.11 networks, there is a need to include non-IEEE 802.11 sources in addition to the IEEE 802.11 nodes contending for the medium in a network. Our contributions to allow an accurate prediction of latency and throughput in the presence of an interfering source are twofold: First, we present an analytical model for an IEEE 802.11 network that includes the previously defined non-IEEE 802.11 interfering source as an extension to the model of Pham [9]. The stations' packet queue behavior is modeled by means of a QBD process. This model allows the prediction of the latency and throughput in a network with interference. Our model focuses on single-hop networks; multi-hop networks are not under consideration.

The second contribution of this paper consists of the verification of the model with simulation and real-life experiments. While simulation offers us a straightforward validation, it can not include all effects that are occurring in reality. As we will see later, the values for latency and throughput do not always align with simulation, especially in the case of significant interference. For this reason, validation in a real scenario is of utmost importance.

The remainder of the paper is organized as follows. First, we present related work in Section 2, then we describe the analytical model in Section 3, which is followed by the description of the queuing model in Section 4. In Section 5, we validate our model against real-life measurements regarding latency and throughput. Finally, we conclude in Section 6.

2. Related work

With the rise of IEEE 802.11 since the late 90s, modeling the network performance became more urgent in order to predict the behavior of the network. One of the most prominent contributions for modeling IEEE 802.11 behavior is the work of Bianchi [1,10]. It models the throughput in the saturated case, using a Markov chain to describe the process of the IEEE 802.11 transmission mechanism. This work has some shortcomings, however. It does not consider the retry limit for sending a packet and therefore, also does not consider dropped packets. An extension was proposed to correct the retry limit and take dropped packets into account as well, while also proposing an improved access method [11]. This model, and especially the Markov chain, serves as a basis for a model describing the average packet latency in an IEEE 802.11 network [12]. Chatzimisios et al. [13] describe how to include the bit error rate simply and straightforwardly [13]. A new Markov chain for the back-off algorithm is proposed and evaluated against an extended version of the existing one [14]. It also corrects an inaccuracy in the work of Chatzimisios et al. [12], where it is assumed that the transmission slot time duration is equal to the average time duration of deferred slots [12]. Including not only latency, but also drop probability, average drop time, and the retry limit, an extended model is presented [15]. A model for latency distribution follows and Distributed Coordination Function (DCF) is analyzed, concluding that it is prone to long latency [16]. A model for channel latency and jitter is presented for the saturated case by Li et al. [17]. This work also includes a discussion about the initial CW the maximal back-off stage and the packet size on the latency. A more advanced latency model for a saturated channel, that also includes jitter and latency distribution as well as drop probability was proposed [18]. A three-dimensional Markov chain, which includes heterogeneous node transmit power levels, is proposed to describe throughput performance under saturation condition [19]. Pham [9] as well as Tickoo and Sikdar [20] and Challa et al. [21] present extensions of the models of Bianchi [10] and Haitao Wu et al. [11] for the unsaturated case [9–11,20,21]. These include latency, as well as throughput, and are based on a queuing model for the packet buffer. Another extension for the unsaturated case is presented by Daneshgaran et al. [22]. This model includes an error-prone channel, while previously an ideal channel was assumed. The analysis for the channel is limited to the bit error probability though. A queue state-driven analysis for ad-hoc networks was proposed, which focuses on end-to-end latency [23]. Saturated and unsaturated cases do not have to be disconnected from each other, as shown by Felemban and Ekici [24]. Here an extension to both cases is presented which focuses on more accuracy in the case of latency and throughput. Similar, with focus on both cases, a model for Quality of Service (QoS) metrics, especially for real-time applications, is proposed [25]. Xu et al. [26] also focus on QoS by maximizing throughput in their model [26]. That computation time is also a factor to consider is shown as well [27]. The authors show that there is a trade-off between accuracy and speed and present one model that is fast, but less accurate and one model that is accurate, but slower. While the previously presented articles focus on direct communication, Xie et al. [28] explore the performance for latency, jitter, and packet loss in a multi-hop ad-hoc network [28]. Mehrnoush et al. [29] extend the model of Bianchi [1] for LTE coexistence experiments by including the ED threshold so that it can be fine-tuned.

To summarize, analytical models consider many QoS parameters, but current analytical models do not take a non-IEEE 802.11 interfering source into account and therefore cannot characterize network performance, such as latency and throughput, accurately in the presence of such a source.

3. Analytical model

In this section, we present a model describing the behavior of an IEEE 802.11 DCF network in the presence of an interfering source. The model covers both the unsaturated and the saturated case. We first give an overview of the model of Pham [9] and then describe our proposed extension.

3.1. Background: Pham's model

Nearly all latency and throughput models for IEEE 802.11 are based on the model of Bianchi [1]. The model of Pham [9], on which we base our model, is also based on the model of Bianchi [1]. It extends the original model from the saturated to the unsaturated case by introducing several new states. There are two main differences; both represented in Fig. 1. First, it includes the case that after the last re-transmission, the packet is dropped and not transmitted, including the post-back-off, which also consumes service time. Second, the unsaturated case, i.e., where the packet queue may be empty, is modeled as well.

The first extension is covered by introducing a transition from the last back-off stage to the post-back-off mechanism. The transition is similar to the standard back-off mechanism but is handled with the minimum contention window and is only applied when the channel has been idle before, and no packet is ready to transmit. This approach preserves the DCF algorithm and avoids a longer back-off as soon as a packet is available for transmission. In Fig. 1, these are the states $(0', j)$, with $j = 0, \ldots, W_0 - 1$. The unsaturated case is handled by introducing an idle

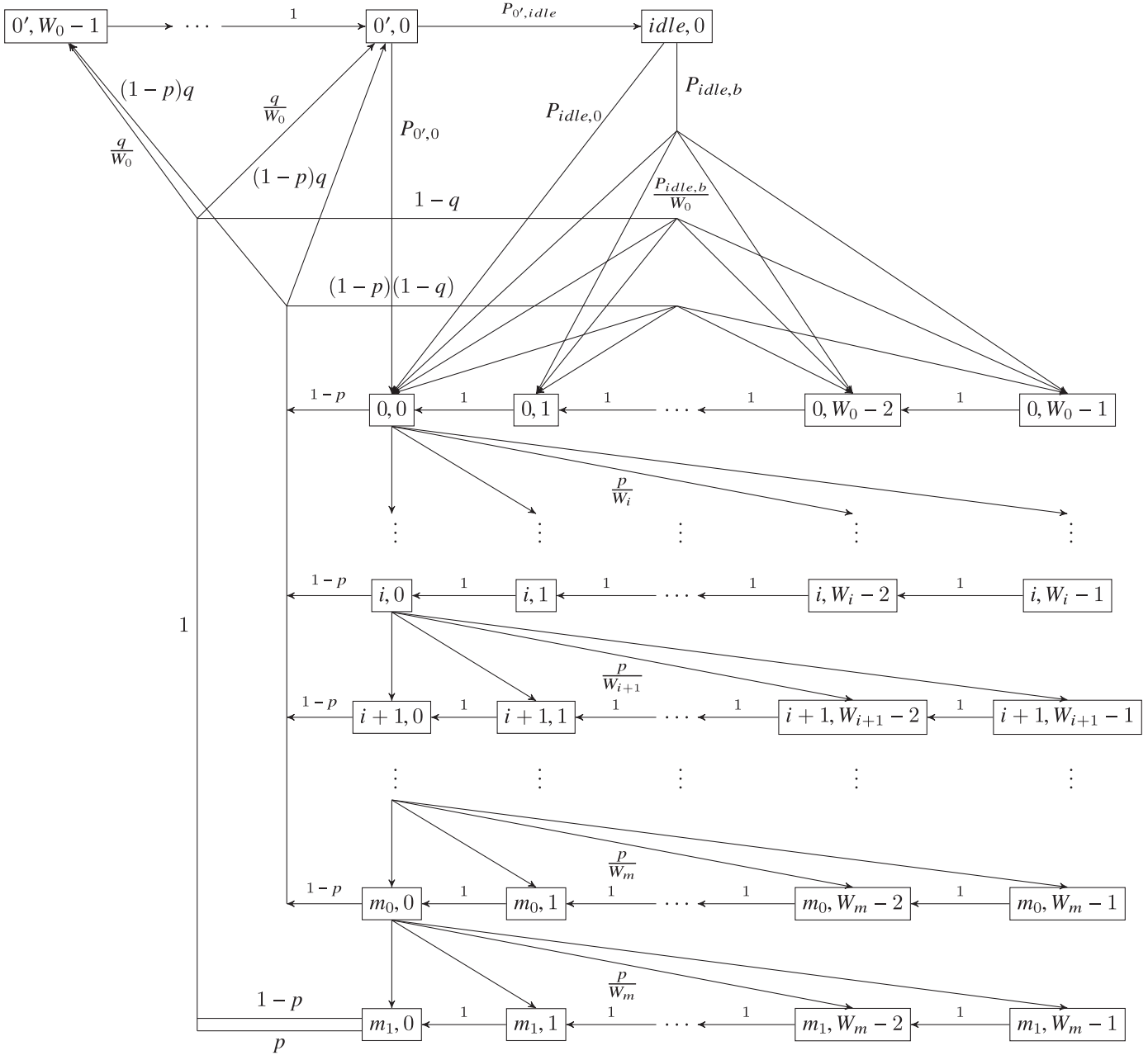

Fig. 1. Transition probabilities $\{s(t), b(t)\}$ of the Markov Chain.

state, $S_{idle,0}$, that can be entered if there is no packet at the head of the queue. If a packet becomes available, depending on the state of the channel, it can be transmitted immediately, with probability $P_{idle,0}$, or it needs to enter the normal back-off phase with $P_{idle,b}$.

3.2. Extension of Pham's model

Consider a slotted system where the length of a slot corresponds to the time slot of the IEEE 802.11 system under study, denoted by σ. We assume that the interfering source only becomes active at the start of a slot. This assumption is mainly made to make the model more manageable. Later experiments do not follow this assumption but still achieve high accuracy. We use the following model for the interfering source. Let

- P_{if} : the probability that at the start of a slot the interfering source becomes active.
- T_{if} : the average duration in multiples of σ that the interfering source is active above the threshold (and hence detected by the stations). We assume that this duration expressed in multiples of the interval σ is geometrically distributed. As a consequence of these assumptions, there is always at least one time-interval σ between two active periods of the interfering source.

The fraction of the time the interfering source is active is given by:

$$P_a = \frac{T_{if}}{T_{if} + \frac{1}{p_{if}}} \tag{1}$$

This general and straightforward model of an interference source allows us to model different sources of interference, independent of the specific communication technology, RF interference, or devices such as microwaves. The parameterization entirely depends on which type of source one wants to model.

Gollakota et al. [30] show that a microwave exhibits a periodical ON-OFF pattern, where the ON period typically lasts for about 10ms and the OFF period for 6 ms [30]. This behavior is confirmed by Hithnawi et al. [31], where the respective durations are 5 ms ON and 15 ms OFF [31]. Gummadi et al. [32] also confirms the results, but do not provide a specific model for the interfering source besides a simple Signal-to-Interference-plus-Noise Ratio (SINR) based one [32].

Also, the presence of a Bluetooth network may interfere with an IEEE 802.11 network. Bluetooth uses a *Frequency Hopping* scheme, and interference may only occur when there is an overlap in time and frequency. A study is made in several papers, among which is the work of Conti et al. [33] and Jung-Hyuck Jo and Jayant [33,34]. The duration of a Bluetooth slot is 625 μs, while the transmission time within a time slot is 366 μs. In order to have interference, there should be a frequency overlap. When e.g., using IEEE 802.11b, the probability that the Bluetooth piconet hops into the IEEE802.11 Direct-Sequence Spread Spectrum (DSSS) passband is 0.25. If the Bluetooth piconet carries a telephone conversation, then 33% of the time slots are used to transmit a packet. Hence the probability that an ON period starts is given by 0.05, and the duration is 366μs.

According to Gollakota et al. [30], digital cordless telephones continuously transmit packets, and therefore the channel is never free for the duration of the call (hence OFF = 0 ms) [30].

Some video monitoring systems use several channels in the 2.4 GHz band. If the camera does not transmit continuously, but one image every xms, then the interference will exhibit an ON-OFF pattern. Hithnawi et al. [31] describe a wireless camera that hops within the frequency range [2.42 GHz–2.45 GHz] [31]. Fig. 3e, in their work, clearly shows the ON-OFF pattern of this camera. The digital Frequency-Hopping Spread Spectrum (FHSS) cordless phone in that paper exhibits a similar ON-OFF pattern.

Shuaib et al. [35] investigate the interference of Zigbee (IEEE 802.15.4) on IEEE 802.11g (and vice versa) [35]. There is no model given for the Zigbee interferer, so we do not know whether the ON-OFF model can be used. Huo et al. [36] investigate the cross-interference of Zigbee and IEEE 802.11 as well, but based on a Packet Error Rate (PER) model and not a signal interference model [36]. In both cases, a further literature study is required.

Bicakci and Tavli [37] present different physical layer attacks that impact the performance of IEEE 802.11 [37]. While our model can not describe all of them, some require sensing capabilities; others can be described by our formulation. Especially the *Hit and Run* tactic they present can be described accurately by our model.

The activity of the interfering source is entirely independent of the operation of the IEEE 802.11 MAC. When the interfering source becomes active while a packet is transmitted, the packet is considered lost, similar to a collision between two packets. If a station has a packet ready for transmission and the interfering source is active, the station will refrain from sending and react as if another station would be active. Like in the case of another IEEE 802.11 station, when the interfering source becomes active, the countdown process of the back-off counter stops until the channel is not considered busy any longer when a station is in a back-off phase. This freezing of the counter is the default behavior of an IEEE 802.11 station.

In this paper, the behavior of a tagged station is modeled employing a QBD process, namely a finite capacity queue with Poisson arrival process and hyperexponential service time [38,39]. The input rate is the arrival rate of packets at the tagged station. The service rate should take into account both the packet transmission and the access delay due to the DCF access mechanism of the IEEE 802.11 MAC. Similar to previous works, the DCF access mechanism is modeled as a Markov Chain, as depicted in Fig. 1. We use an adaptation of the IEEE 802.11 DCF MAC model proposed by Pham [9]. Consider an IEEE 802.11 network with n stations and let for a tagged station at time t

- $b(t)$: the back-off time counter
- $s(t)$: the back-off stage $(0, \dots, m+1)$

We use similar notations as Pham [9], which can be seen in Table 1 [9].

Table 1
Summary of parameters.

Parameter	Description
p	Probability of packet not received
τ	Probability of station sending in randomly chosen slot
ω	Probability that FEC mechanism can correct the packet
q	Probability of empty queue
$b(i, j)$	Probability of node in backoff state $S_{i,j}$
$b(idle, 0)$	Probability of node in idle state $S_{idle,0}$
$P_{0',0}$	Probability to send immediately after post-back-off
$P_{idle,0}$	Probability to send immediately after idle state
$P_{idle,b}$	Probability to send after back-off after idle state
$P_{0',idle}$	Probability to go into idle state after post-back-off
$P_{tr(n)}$	Probability that at least one out of n nodes transmits
$P_{s(n)}$	Probability that one out of n nodes transmits successfully
$P_{tr(n-1)}$	Probability that at least one out of $n-1$ nodes transmits
$P_{s(n-1)}$	Probability that one out of $n-1$ nodes transmits successfully
P_l	Probability that packet is lost due to overflow in queue
$S_{i,j}$	State of node when $s(t) = i$ and $b(t) = j$
$S_{idle,0}$	State of node when no packet ready for transmission
W	Minimal backoff window size
W_i	Backoff window size at stage $s(t) = i$
σ	Channel idle slot (system slot)
$\bar{\sigma}$	Average channel slot time
λ	Average packet arrival rate
μ	Packet processing rate
Q_l	Queue length
δ	Propagation latency
U	Average throughput of station
$E[A]$	Average latency of packet

3.3. Derivation of parameters in a system with interfering source

We consider the 2-dimensional stochastic process $\{s(t), b(t)\}$, of which the transition probabilities are given in Fig. 1. The states (i, j), with $i = 0, \dots, m+1$ and $j = 0, \dots, W_i - 1$, correspond to those of the saturated case (see Bianchi and Raptis et al.) [10,18]. The states $(0', j)$, with $j = 0, \dots, W_0 - 1$, represent the post-back-off mechanism, and the state $(idle, 0)$ represents the state where the queue of the tagged station is empty. These additional states are needed to model an unsaturated network

We define two key parameters for our model, p and τ. Let τ be the probability that a station starts sending a packet in a randomly chosen time slot and let p be the probability that the transmission of a packet is not successful. Additionally, we define ω being the probability that during an ongoing packet transmission, the interfering source becomes active, but this does not lead to the loss of a packet, as the FEC mechanism of the Physical Layer (PHY) is able to correct the corrupted bits due to the collision. The derivation of these first two parameters are based on the steady-state of the Markov chain $s(t)$, $b(t)$ and are computed in the next section. Once p and τ are known it is possible to define the following parameters: $P_{tr(n)}$ and $P_{tr(n-1)}$ being the probabilities that at least one out of n or $n-1$ stations transmits respectively and $P_{s(n)}$ and $P_{s(n-1)}$ being the probabilities that there is a successful transmission out of n or $n-1$ stations respectively. It is clear that

$$\begin{aligned} P_{tr(n)} &= 1 - (1-\tau)^n \\ P_{tr(n-1)} &= 1 - (1-\tau)^{n-1} \\ P_{s(n)} &= n \cdot \tau(1-\tau)^{n-1} \\ P_{s(n-1)} &= (n-1) \cdot \tau \cdot (1-\tau)^{n-2} \end{aligned} \tag{2}$$

$P_{0',0}$ describes the probability to move from state $S_{0',0}$, after the post-back-off, to state $S_{0,0}$, meaning a direct transmission, if there is a packet ready for transmission at the station. If there is no packet, the station

moves to state $S_{idle,0}$ with probability $P_{0',idle}$. Similar, if the station is in state $S_{idle,0}$, a packet arrives, and the channel has been idle for more than DCF Interframe Space (DIFS), the packet is transmitted immediately with probability $P_{idle,0}$. Otherwise, the node enters into a back-off state $S_{0,i}$, $0 \leq i \leq W_0 - 1$ with probability $P_{idle,b}$.

The probabilities for $P_{0',0}$ and $P_{0',idle}$ stay the same as in the work of Pham [9]:

$$P_{0',0} = 1 - e^{\frac{-\lambda W_0 \widetilde{\sigma}}{2}} \tag{3}$$

and

$$P_{0',idle} = e^{\frac{-\lambda W_0 \widetilde{\sigma}}{2}} \tag{4}$$

Both $P_{idle,0}$ and $P_{idle,b}$ need to be changed to include the interfering source. When the station is in the idle state, then a transition towards state $S(0, 0)$ occurs in two cases:

- There is an arrival before the first DIFS period ends and during that DIFS period there are no other stations that start to transmit and the interfering source is not active (i.e., the source was not active at the start of the DIFS period and moreover, does not become active during the DIFS period). The probability for this event equals

$$\left(1 - e^{-\lambda DIFS}\right) \cdot \left[(1 - p_{if})(1 - \tau)^{n-1}\right]^{\frac{DIFS}{\sigma}} \tag{5}$$

- The first arrival at the tagged station occurs after the first DIFS period ends, and during the time-interval the station was idle. The medium has been sensed idle (i.e., no other station has started to transmit, and the interfering source has not been active, i.e., the source was not active at the start of the idle period and moreover, has not become active during that period). In that case, the packet is sent immediately, i.e., a transition to state $S(0, 0)$ occurs. The probability for this event equals

$$e^{-\lambda DIFS}\left[(1 - p_{if})(1 - \tau)^{n-1}\right]^{\frac{DIFS}{\sigma}}\left(1 - e^{-\lambda\sigma}\right)\sum_{t=0}^{\infty} e^{-\lambda\sigma t}\left[(1 - p_{if})(1 - \tau)^{n-1}\right]^{t} \tag{6}$$

Hence

$$\begin{aligned} P_{idle,0} = {} & \left(1 - e^{-\lambda DIFS}\right)\left[(1 - p_{if})(1 - \tau)^{n-1}\right]^{\frac{DIFS}{\sigma}} \\ & + e^{-\lambda DIFS}\left[(1 - p_{if})(1 - \tau)^{n-1}\right]^{\frac{DIFS}{\sigma}}\left(1 - e^{-\lambda\sigma}\right) \\ & \times \sum_{t=0}^{\infty} e^{-\lambda\sigma t}\left[(1 - p_{if})(1 - \tau)^{n-1}\right]^{t} \end{aligned} \tag{7}$$

and

$$P_{idle,b} = 1 - P_{idle,0} \tag{8}$$

The states $S(m, j)$ and $S(m + 1, j)$ with $0 \leq j \leq W_m - 1$ are the last two stages of the back-off mechanism. In stage $S(m + 1, j)$ the packet is either transmitted or discarded. The CW of the last two stages W_m and W_{m+1} both equal the maximum window size of $2^m W_0$.

We denote by q the probability that the transmission queue in the tagged station is empty. This value is determined in Section 4.

3.4. Derivation of the steady-state probability

In what follows, we describe the steady-state probabilities of the Markov chain as a function of $b_{(0,0)}$. We follow the same reasoning as Pham [9] and obtain [9]

$$\begin{aligned} D_1 = {} & \frac{1}{2} \cdot \left[W \cdot \left(\sum_{i=1}^{m} (2p)^i + p \cdot (2p)^m \right) + \frac{p \cdot (1 - p^{m+1})}{1 - p} \right] \\ & + q \cdot \left(\frac{2 \cdot P_{0'0} + W + 1}{2} \right) \end{aligned} \tag{9}$$

$$D_2 = \frac{q \cdot P_{0',idle}(P_{idle,0} + 1)}{P_{idle,0} + P_{idle,b}} + \frac{(W + 1) \cdot \left(\frac{q \cdot P_{0',idle} P_{idle,b}}{P_{idle,0} + P_{idle,b}} + (1 - q) \right)}{2} \tag{10}$$

$$b(0, 0) = \frac{1}{D_1 + D_2} \tag{11}$$

3.5. Derivation of channel slot time with an interfering source

As a next step, we need to calculate $\widetilde{\sigma}$, the average channel slot time. This time includes the average time the channel is idle, or busy with a packet transmission or collision. Besides the fixed times for DIFS and SIFS, we need three other times. The average channel slot time σ, the time for a successful transmission T_s, and the time for a collision T_c. We consider two cases: the basic scheme and the scheme using Request-To-Send/Clear-To-Send (RTS/CTS). These can be derived as follows:

$$T_s = P_L + SIFS + \delta + ACK + DIFS + \delta \tag{12}$$

and

$$T_c = P_L + DIFS + \delta \tag{13}$$

with

$$P_L = T_{preamble} + T_{signal} + N_{SYM} \cdot \left\lceil \frac{16 + 8 \cdot (P_B + H) + 6}{N_{DBPS_{DATA}}} \right\rceil \tag{14}$$

and

$$ACK = T_{preamble} + T_{signal} + N_{SYM} \cdot \left\lceil \frac{16 + 8 \cdot 14 + 6}{N_{DBPS_{CON}}} \right\rceil \tag{15}$$

where the transmission time for the preamble, $T_{preamble} = 16$ µs, the transmission time for the signal, $T_{signal} = 4$ µs, and the transmission time for a symbol, $N_{SYM} = 4$ µs in a 20 MHz channel when using the Orthogonal Frequency-Division Multiplexing (OFDM) PHY, which we use later on in our experiments. $N_{DBPS_{DATA}}$, the transmitted bytes per symbol for data, depends on the data rate used as well as $N_{DBPS_{CON}}$, the transmitted bytes per symbol with the control rate. P_B is the packet length in bytes, while H is the length of the header.

When the RTS/CTS mechanism is used, T_s and T_c are the following

$$T_s = RTS + SIFS + \delta + CTS + SIFS + \delta + P_L + \delta + ACK + DIFS + \delta \tag{16}$$

and

$$T_c = RTS + DIFS + \delta \tag{17}$$

with

$$RTS = T_{preamble} + T_{signal} + N_{SYM} \cdot \left\lceil \frac{16 + 8 \cdot 20 + 6}{N_{DBPS_{CON}}} \right\rceil \tag{18}$$

and

$$RTS = T_{preamble} + T_{signal} + N_{SYM} \cdot \left\lceil \frac{16 + 8 \cdot 14 + 6}{N_{DBPS_{CON}}} \right\rceil \tag{19}$$

Let parameter k be:

$$k = \left\lceil \frac{T_s}{\sigma} \right\rceil \tag{20}$$

and l respectively:

$$l = \left\lceil \frac{T_c}{\sigma} \right\rceil \tag{21}$$

denoting the number of time slots for T_s and T_c.

To calculate the average channel slot time $\widetilde{\sigma}$, we need to take the presence of the interfering source into account. The average channel slot time $\widetilde{\sigma}$ consists of the following components:

- No other packet is sent, and the interfering source does not become active at the start of this slot. In that case, the contribution to $\widetilde{\sigma}$ equals:

$$(1 - P_{tr(n-1)}) \cdot (1 - p_{if}) \cdot \sigma \tag{22}$$

- The interfering source becomes active at the start of this slot, and the tagged station considers the channel busy. In that case, the contribution to $\widetilde{\sigma}$ equals:

$$p_{if} \cdot (T_{if} + \sigma) \tag{23}$$

- A packet is sent successfully; thus, the interfering source does not become active during $k+1$ time-intervals of length σ, or does become active, but the FEC solves the problem. In that case, the contribution to $\widetilde{\sigma}$ equals:

$$P_{s(n-1)} \cdot \left[(1-p_{if})^{k+1} \cdot (T_s + \sigma) + \sum_{j=0}^{k-1} (1-p_{if})^j \cdot p_{if} \cdot \omega \cdot (T_s - j \cdot \sigma + T_{if} + \sigma) \right] \tag{24}$$

This results into

$$P_{s(n-1)} \cdot \left[(1-p_{if})^{k+1} \cdot (T_s + \sigma) + \omega \cdot \left((1-(1-p_{if})^{k+1}) \cdot (T_s + T_{if} + \sigma) - \sigma \cdot (1-p_{if}) \cdot \frac{1-(1-p_{if})^{k-1} \cdot (1+(k-1) \cdot p_{if})}{p_{if}} \right) \right] \tag{25}$$

- A packet is sent successfully, and the interfering source does not become active during transmission, but it becomes active in the time-interval immediately following the successful transmission, and the tagged station considers the channel busy. In that case, the contribution to $\widetilde{\sigma}$ equals:

$$P_{s(n-1)} \cdot (1-p_{if})^k \cdot p_{if} \cdot (T_s + T_{if} + \sigma) \tag{26}$$

- A packet is sent but involved in a collision with another packet we assume that the interfering source does not become active during the interval of length T_c. The tagged station considers the channel busy. In that case, the contribution to $\widetilde{\sigma}$ equals:

$$P_{tr(n-1)} \cdot \left(1 - \frac{P_{s(n-1)}}{P_{tr(n-1)}} \right) \cdot (1-p_{if})^{l+1} (T_c + \sigma) \tag{27}$$

- A packet is sent but involved in a collision with another packet; we assume that the interfering source does not become active during the interval of length T_c. Moreover, the interfering source becomes active in the time-interval immediately following the time-interval T_c. The tagged station considers the channel busy. In that case, the contribution to $\widetilde{\sigma}$ equals:

$$P_{tr(n-1)} \cdot \left(1 - \frac{P_{s(n-1)}}{P_{tr(n-1)}} \right) \cdot (1-p_{if})^{l} \cdot p_{if} \cdot (T_c + T_{if} + \sigma) \tag{28}$$

- A packet is sent but involved in a collision with the interfering source that can not be solved by the FEC mechanism (the interfering source does not become active at the start of the time-interval because Eq. (23) covers this), and the tagged station considers the channel busy. In that case, the contribution to $\widetilde{\sigma}$ equals (remark that Eq. (26) covers the case $n = k$):

$$P_{s(n-1)} \cdot \left(\sum_{j=1}^{k-1} (1-p_{if})^j \cdot p_{if} \cdot (1-\omega) \cdot (j \cdot \sigma + T_{if} + \sigma) \right) \tag{29}$$

- A packet is sent but involved in a collision with another packet and in a collision with the interfering source (the interfering source does not become active at the start of the time-interval because Eq. (23) covers this), and the tagged station considers the channel busy. In that case, the contribution to $\widetilde{\sigma}$ equals (remark that Eq. (28) covers the case $n = l$):

$$P_{tr(n-1)} \cdot \left(1 - \frac{P_{s(n-1)}}{P_{tr(n-1)}} \right) \cdot \left(\sum_{n=1}^{l-1} (1-p_{if})^n \cdot p_{if} \cdot (n \cdot \sigma + T_{if} + \sigma) \right) \tag{30}$$

Subsequently, $\widetilde{\sigma}$ is the sum of all those components. Note that this leads to a different formula compared to Pham [9], which leads to different results between our model and the original one from Pham [9] (see Section 5) [9].

3.6. Derivation of p and τ

The values for p and τ can only be derived numerically. For this purpose, we need two independent formulas for τ. The first one can be formulated following the Markov chain by using the state $b(0, 0)$, defined in Eq. (11):

$$\tau = \sum_{i=0}^{m_1} b(i,0) = \frac{b(0,0) \cdot (1-p^{m+2})}{1-p} \tag{31}$$

The second one can be derived directly from the definition of p, which is equal to all possibilities of at least two stations transmitting and the probability that the interfering source is active:

$$p = 1 - (1-\tau)^{n-1} [(1-p_{if})^k + (1-(1-p_{if})^k) \cdot \omega] \tag{32}$$

which we can rewrite as:

$$\tau = 1 - \sqrt[n-1]{\frac{p-1}{\omega(1-p_{if})^k - (1-p_{if})^k - \omega)}} \tag{33}$$

Using Eqs. (31) and (33), we can derive p and τ numerically.

3.7. Throughput

The throughput of a station can be derived directly from a successful transmission by a station. A successful transmission is composed of the probability that only one station transmits, $\tau(1-\tau)^{n-1}$, the probability that the interfering does not become active during the transmission or that it becomes active but does not lead to packet loss due to the presence of the FEC mechanism, being $(1-p_{if})^{k+1} + \omega \cdot (1-(1-p_{if})^{k+1})$, and the probability that the station has a packet at the head of the queue $(1-q)$. As the throughput is defined as the fraction of the channel slots being used, we can write the channel throughput U as:

$$U = \frac{P_B \cdot \tau(1-\tau)^{n-1}(1-q)((1-p_{if})^{k+1} + \omega \cdot (1-(1-p_{if})^{k+1}))}{\widetilde{\sigma}} \tag{34}$$

4. The M/HEXP/1/Q queuing model

In what follows, we model a station as a queue with Poisson input, hyperexponential service time, and finite buffer capacity [39].

Packets arrive according to a Poisson process with rate λ. Upon arrival they join a finite queue with capacity Q. Packets arriving at a full queue are lost. Accepted packets are transmitted in a First-In, First-Out (FIFO) order.

We distinguish between $m+2$ types of packets:

- Type i packets $0 \le i \le m+1$ are transmitted after i unsuccessful transmissions: given the definition of the parameter p, a packet belongs to type i, $0 \le i \le m-1$, with probability $a_i = p^i \cdot (1-p)$. Its mean service time, i.e., the time between the packet is at the head of the queue and starts competing for accessing the medium and the time instant the transmission starts, is given by

$$E[A]_i = T_s + i \cdot T_{col} + \widetilde{\sigma} \cdot \sum_{j=0}^{i} \frac{W_i - 1}{2} \tag{35}$$

with T_{col} given by

$$T_{col} = (1-p_{if})^l \cdot T_c + \sum_{b=1}^{l} (1-p_{if})^{b-1} \cdot p_{if} \cdot (\sigma \cdot (b-1) + T_{if}) \tag{36}$$

- Type $m+2$ packets are lost due to the contention process (collision with packets of other stations or with the interfering source).

A packet belongs to type $m+2$ with probability $a_{m+2} = p^{m+2}$. The mean access delay of this type of packet is given by

$$E[A]_{m+2} = (m+2) \cdot T_{col} + \widetilde{\sigma} \cdot \sum_{j=0}^{m+1} \frac{W_j - 1}{2} \tag{37}$$

Remark that type $m+2$ packets are not successfully transmitted, but contribute to the latency of successfully transmitted packets.

These assumptions turn a station into a finite capacity queue with Poisson input and hyperexponential service time, denoted by *M/HEXP/1/Q/* (see Eq. (29)).

This queue is a continuous-time QBD process. The rate matrix G is determined as follows:

Define the following matrices:

B_0 is an $1 \times (m+3)$ matrix with entries

$$(B_0)_{1,i} = a_{i-1} \cdot \lambda \quad , i = 1, \dots, m+3 \tag{38}$$

B_1 is a 1×1 matrix with entries

$$(B_1)_{1,1} = -\lambda \tag{39}$$

B_2 is an $(m+3) \times 1$ matrix with entries

$$(B_2 1)_{i,1} = \mu_{i-1} \quad , i = 1, \dots, m+3 \tag{40}$$

with

$$\mu_i = \frac{1}{E[A]_i} \tag{41}$$

A_0 is an $(m+3) \times (m+3)$ diagonal matrix with diagonal entries

$$(A_0)_{i,i} = \lambda \quad , i = 1, \dots, m+3 \tag{42}$$

A_1 is an $(m+3) \times (m+3)$ diagonal matrix with diagonal entries

$$(A_1)_{i,i} = \lambda + \mu_{i-1} \quad , i = 1, \dots, m+3 \tag{43}$$

A_2 is an $(m+3) \times (m+3)$ matrix with entries

$$(A_2)_{i,j} = a_{j-1} \cdot \mu_{i-1} \quad , i, j = 1, \dots, m+3 \tag{44}$$

The rate matrix G, with dimensions $Q_l \cdot (m+3) + 1 \times Q_l \cdot (m+3) + 1$, is given by

$$\begin{pmatrix} B_1 & B_0 & & & & & & \\ B_2 & A_1 & A_0 & & & & & \\ & A_2 & A_1 & A_0 & & & & \\ & & \ddots & \ddots & \ddots & & & \\ & & & \ddots & \ddots & \ddots & & \\ & & & & \ddots & \ddots & \ddots & \\ & & & & & A_2 & A_1 & A_0 \\ & & & & & & A_2 & A_1 + A_0 \end{pmatrix} \tag{45}$$

The stationary distribution of the number of packets in a station is given by

$$\bar{\nu} = (\bar{\nu_0}, \dots, \bar{\nu_{Q_l}}) \tag{46}$$

where the row vector $\bar{\nu}$ can be calculated by solving the linear system

$$\bar{\nu} G = \bar{o} \tag{47}$$

with normalization condition

$$\bar{\nu} \bar{e} = 1 \tag{48}$$

where $\bar{e}$ is a column vector with all entries equal to 1.

The probability that there are i packets in a station, $i \leq i \leq Q_l$, is given by

$$\begin{aligned} \pi_0 &= \bar{\nu_0} \\ \pi_i &= \bar{\nu_i} \bar{e_i} \end{aligned} \tag{49}$$

where $\bar{e_i}$ is a column vector of dimension $m+3$ with all entries equal to 1. Remark that $\bar{\nu_0}$ is a scalar. Solutions of finite QBD processes are discussed in‘[38]. Remark that $q = \pi_0$ (i.e., the probability that the queue is empty).

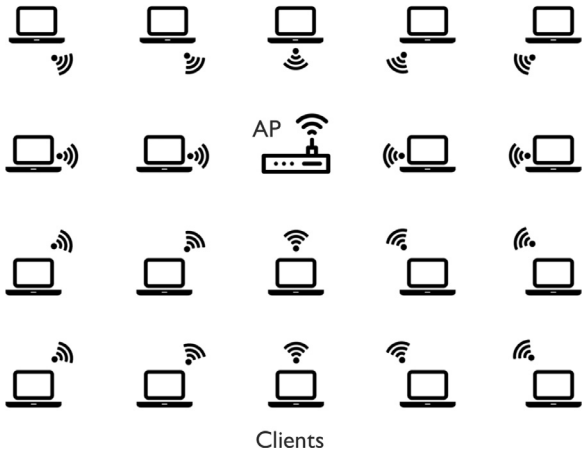

Fig. 2. Setup of experiment with central access point and clients around it.

The mean number of packets in a station is given by

$$E[S] = \sum_{i=0}^{Q_l} i \cdot \pi_i \tag{50}$$

moreover, the mean number of packets in the queue of a station is given by

$$E[QL] = \sum_{i=1}^{Q_l} (i-1) \cdot \pi_i = E[S] - (1 - \pi_0) \tag{51}$$

The mean time a packet (successfully transmitted or not) spends in the queue is, using Little's formula, given by

$$\frac{E[QL]}{\lambda(1 - \pi_Q)} \tag{52}$$

Remark that in this queue both packets of type i, $0 \leq i \leq m+1$, and packets of type $m+2$ are present. However, to derive the total mean access latency a packet experiences (i.e., both queuing and service time), only successfully transmitted packets need to be taken into account. Therefore, the mean packet access latency is given by

$$E[A] = \frac{E[L]}{\lambda \cdot (1 - \pi_Q)} + \sum_{i=0}^{m+1} E[A]_i \cdot \frac{p^i \cdot (1-p)}{1 - p^{m+2}} \tag{53}$$

5. Results

In this section, we describe the setup for our measurements and present results for latency and throughput. We compare our model against an established model in the case of no interference and simulation and measurements in the case of interference.

5.1. Setup and parameters

For our results, we have three different scenarios, simulation, measurements in a real testbed, and the model.

For our real measurements, the w-ilab.t[1] lab facility, a large-scale emulation platform with wireless nodes allowing extensive experiments, has been used. For our configurations, we were limited to 15, 20, and fixed 25 stations on the 5 GHz band. All stations are connected to a central access point (AP) (as seen in Fig. 2) and are sending packets to it over a time of 60 s. Packets are sent on the MAC layer to reduce the impact of any higher layer. The AP is forced to use IEEE 802.11a, enforcing the use of the OFDM PHY, and IEEE 802.11n capabilities are disabled. The packets have a size of 1530 bytes and are sent at a fixed bit rate of 54 Mbps. The number of packets per seconds starts at 25

[1] http://doc.ilabt.imec.be/ilabt-documentation/index.html.

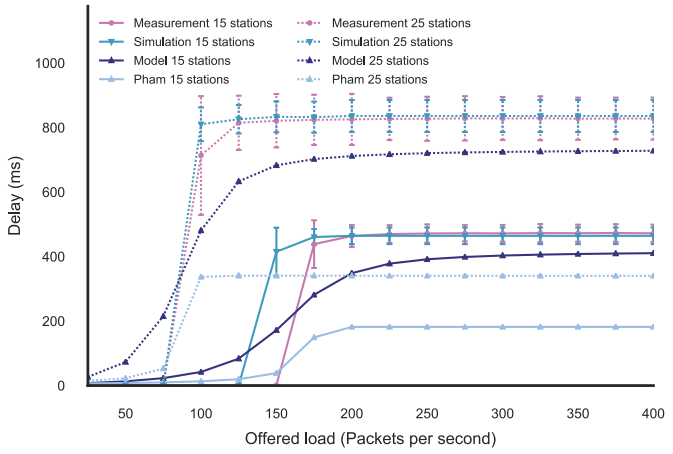

Fig. 3. Latency comparison with no interference between simulation, measurements, our new model, and Pham's model for 15 and 25 stations.

and increments by steps of 25 packets per second up to 400 packets per second. Each configuration was repeated five times.

Additionally, we installed a Software Defined Radio (SDR) to generate interference according to the model of an interfering source defined in Section 3. The SDR is not time-aligned with the slots of the IEEE 802.11 system and therefore completely decoupled, which is a more realistic scenario but is contrary to one assumption for the model. The stations are of type Zotac Zbox ID10 with IEEE 802.11n capable wireless cards, the AP consists of a PC Engines APU 1d4 with an IEEE 802.11ac enabled wireless card, and the SDR is a USRP N210.

Additionally, we used simulation as a second comparison besides real measurements. We implemented the interfering source in *ns3*, version 3.28, and simulated the same scenarios as for the real setup to stay comparable. The interfering source works similar to the already existing waveform generator. Instead of periodic transmission, it works as an on/off source. Each time slot, it turns on with given probability and remains active for the specified amount of time slots. As in the real setup, the interfering source in simulation is not time-aligned to the IEEE 802.11 system. The ED threshold was set to −74dBm, while the Friis propagation loss model and the constant speed propagation delay model were used. The data rate was set to 54 Mbps and the control rate to 6 Mbps, both using OFDM and both at a constant rate.

The parameters for the interfering source were chosen according to a *low occurrence* with $p_{if} = 0.01$ and a *high occurrence* with $p_{if} = 0.025$. The duration can be distinguished between a *low duration* with $T_{if} = 10$, a *medium duration* with $T_{if} = 50$, and a *high duration* with $T_{if} = 100$. Table 3 shows the airtime for each configuration. Higher interference probabilities are not presented, because the measurements are unreliable for very high interference cases as not enough packets are correctly delivered. The rest of the values can be seen in Table 2.

5.2. Latency measurements

For the analysis of the latency, there are two significant points to consider. First, the point when saturation is reached. This point is reached when the latency suddenly goes from a few milliseconds to the maximum possible, which can be up to several seconds. Second, the maximum latency. This maximum is achieved as soon as saturation is reached. Both are essential indications for QoS and determine the quality of the link for a user.

First, we compare the performance of our model with no interference against Phams's [9] model, as well as simulation, and measurements in Fig. 3 [9]. While predicting the saturation point correctly, we can see that Pham's [9] model significantly underestimates latency in both simulation and measurements, by 250%. Our model predicts the saturation

Table 2
Summary of values.

Parameter	Value
W	32
Q_l	64
m	5
Bitrate	54 Mbps
P_B	1530 byte
H	28 byte
δ	10^{-6} s
σ	$9 \cdot 10^{-6}$ s
$T_{preamble}$	$16 \cdot 10^{-6}$ s
T_{signal}	$4 \cdot 10^{-6}$ s
DIFS	$34 \cdot 10^{-6}$ s
SIFS	$16 \cdot 10^{-6}$ s
N_{SYM}	$4 \cdot 10^{-6}$ s
$N_{DBP_{DATA}}$	216
$N_{DBP_{ACK}}$	96

Table 3
Airtime occupation of interfering source for different probabilities and timeslots used in the presented experiments.

p_{if} T_{if}	10	50	100
0.01	9.1%	33.33%	50%
0.025	20%	55.55%	71.43%

point correctly, but still slightly underestimates simulation and measurement by 11%, but in general, performs much better. The difference between our model and Pham's [9] model lies in a different formulation for the average slot time $\widetilde{\sigma}$. We corrected a mistake in Pham's [9] formula. The slightly higher value for the simulation in the case of 25 stations compared to the measurements likely stems from two reasons. First, the fact that in a real setup, not every node hears all transmissions from all other nodes. Second, the exact behavior of IEEE 802.11 hardware and firmware are partially unknown as it is vendor dependent. This black box behavior is especially the case for the ED threshold, which influences the detection of a busy medium. The fact that this happens with 25, but not 15 stations, makes it very likely that not all stations consider the channel busy at the same time.

Fig. 4 gives an overview of the behavior captured by the models in the unsaturated phase in greater detail for 15 and 25 stations. We can see that the model of Pham [9] has a more prolonged phase of lower latency, while our model increases latency early on [9]. Interference amplifies this effect, and with high interference, the latency is increased at around ten packets per second already.

Fig. 5 a and b are the first figures that show interference with the first a low occurrence ($p_{if} = 0.01$), the second a high occurrence ($p_{if} = 0.025$), and both with a medium duration ($T_{if} = 50$). Our model predicts the saturation point correctly independent of the number of stations while the maximum latency is slightly underestimated. In the case of low occurrence, the difference in latency to the measurements is below 9%, while it is below 3% for the simulation. When a high occurrence of interference is present, the model keeps within the 9% range but is further away from the simulation, which is acceptable as the simulation severely underestimates the interference.

In Fig. 6a and b the number of stations is fixed to 25 while we have a low occurrence of interference ($p_{if} = 0.01$) in the first figure and high occurrence ($p_{if} = 0.025$) in the last. In all cases, our model predicts the saturation point accurately. In the case of low occurrence, our model is slightly underestimating both, simulation and measurement, by 3% and 11–14% respectively, with a better result with higher duration ($T_{if} = 100$) when compared to the measurements. In the case of high occurrence, our model is closer to the measurement compared to the simulation, independent of duration. We can achieve a difference

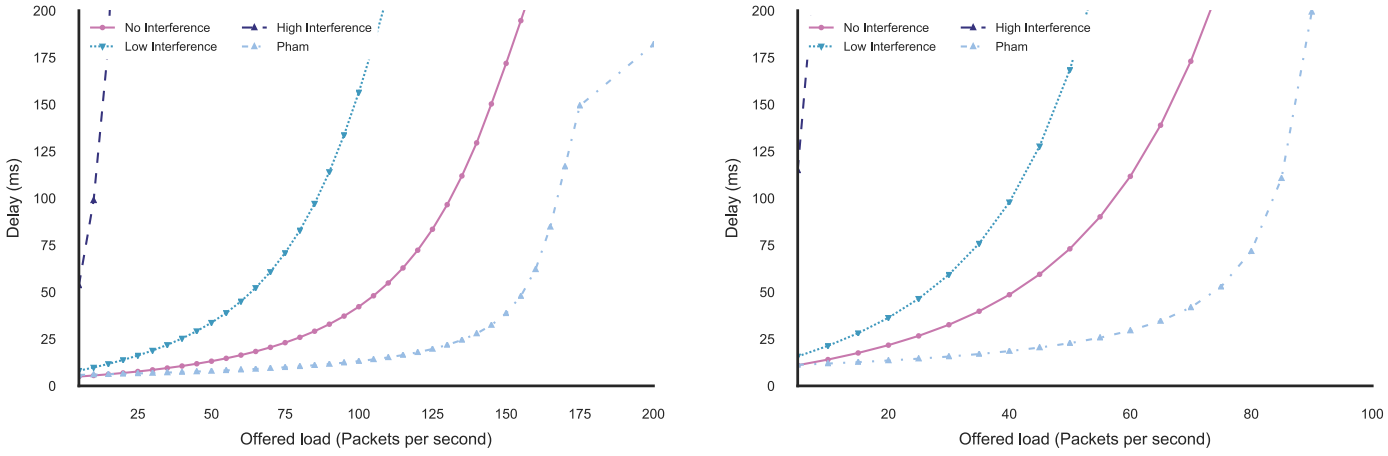

(a) 15 stations. (b) 25 stations.

Fig. 4. Latency comparison of models before saturation for variable interference and fixed number of stations.

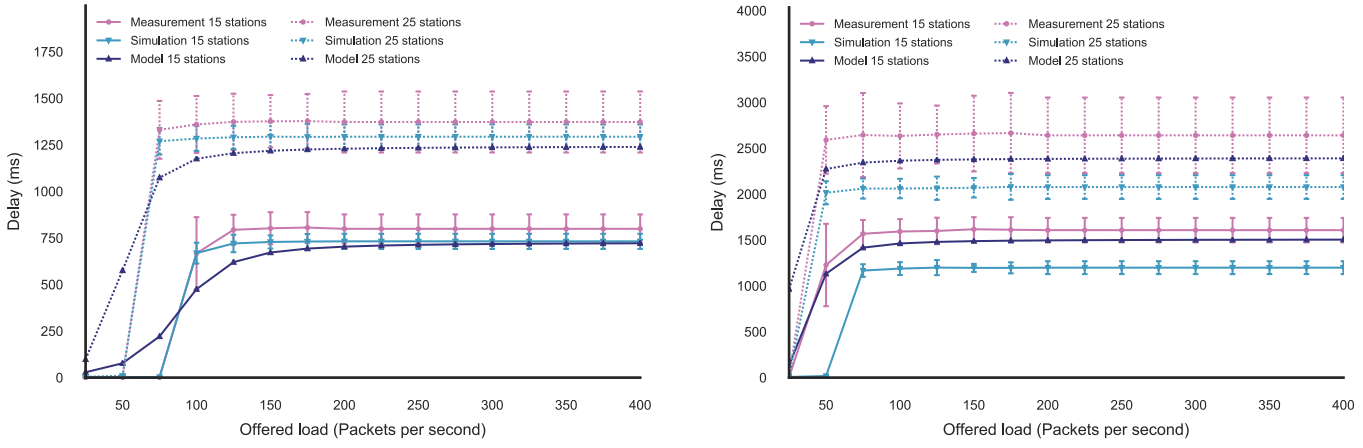

(a) Low interference occurrence and medium duration. (b) High interference occurrence and medium duration.

Fig. 5. Latency for fixed interference occurrence, fixed medium duration, and changing number of stations.

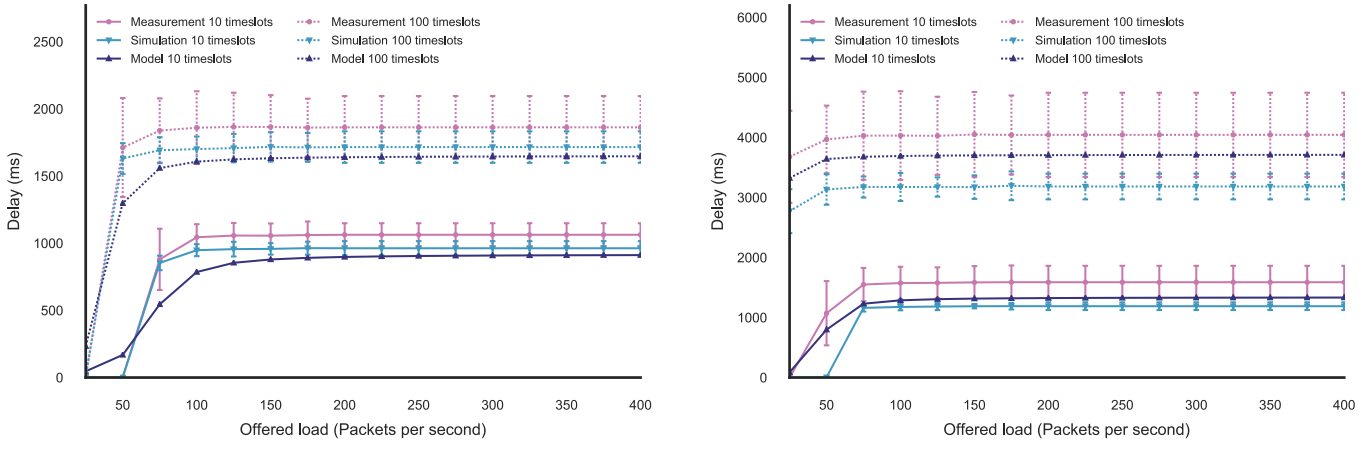

(a) Low interference occurrence and 25 stations. (b) High interference occurrence and 25 stations.

Fig. 6. Latency for fixed interference occurrence, fixed number of stations, and changing duration.

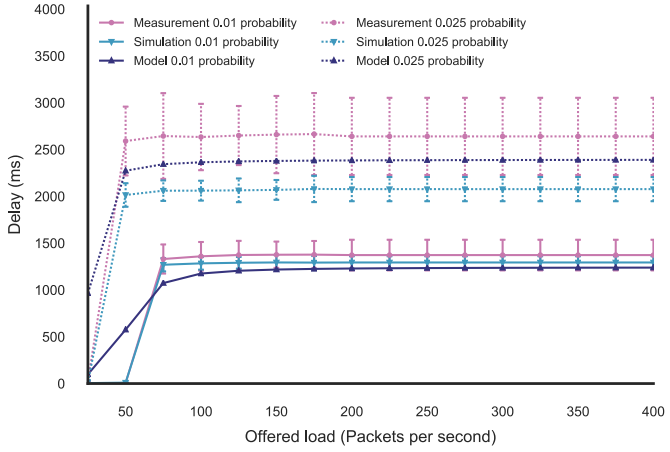

Fig. 7. Latency for medium duration, 25 stations, and changing occurrence.

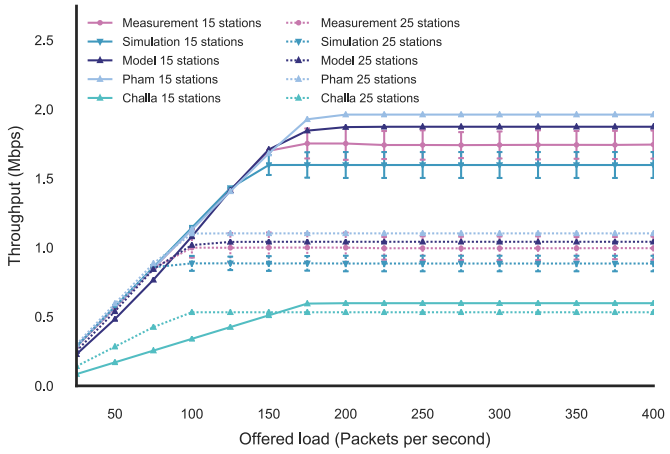

Fig. 8. Throughput comparison with no interference between simulation, measurements, our new model, Pham's [9] model, and Chella et al.'s [21] for 15 and 25 stations [9,21].

compared to the measurement of 8.5-17%, with higher accuracy when the duration is longer. The simulation deviates from the measurements by 27–33%, which shows that the simulation can not fully capture the effect of interference on an IEEE 802.11 network.

Fig. 7 shows a fixed duration, medium ($T_{if} = 50$), with a fixed number of stations (25), and changing occurrences. Our model predicts the saturation point correctly in all scenarios. The latency for low occurrence is jointly estimated by both model and simulation, with 9% and 6% respectively. High occurrence increases this difference, and our model can capture the effects of a real deployment much better than the simulation with a difference of 9% for the model and 27% for simulation.

Our model can accurately predict the latency of a real setup while the simulation is too simplified to cope well with high interference. The results show that our model can, therefore, be used in a setup where QoS is essential, compared to simulation.

5.3. Throughput measurements

Let us now consider the throughput. Again, two significant points are essential. First, the slope at the beginning where the requested bandwidth is still available until the maximum throughput is achieved. This point is similar to the saturation point. Second, the maximum throughput itself that a station can achieve in each scenario.

Fig. 8 compares our model against Pham's [9] model and Chella et al.'s [21]'s model, as well as against simulation and measurement for 15 and 25 stations [9,21]. While our model estimates the slope correctly, both, Pham's [9] model and Chella et al.'s [21] model overestimate the slope and possible throughput for a station significantly. In the first case by 10–11% and the second case by 14–19% [9,21]. Simulation underestimates available throughput by 9–12%, while our model slightly overestimates throughput by 2–4%. Our model outperforms all other models, including simulation.

The difference between our model and Pham's [9] model is the same as in Fig. 3.

The first throughput results with interference can be seen in Fig. 9a with the low occurrence and in Fig. 9b with the high occurrence and medium duration. Simulation and model both follow the slope well while the model underestimates the throughput slightly by 9% and the simulation by 6–9% in the case of low occurrence. When the interference has a high occurrence, the model underestimates slightly by 6–9%, and the simulation overestimates the performance by 27–34%. Again, the simulation represents the effects of reality correctly when the interference has a high occurrence.

Fig. 10 a and b show the effect of a changing duration in combination with different occurrences. If there is low interference occurrence, then both simulation and model are reasonably accurate with 11–14% and 9–10% respectively. The duration itself has not much effect. In the case of high occurrence, the difference is more significant, with 27–33% for simulation and 8–17% for our model with better accuracy when the duration of the interference source is longer.

In Fig. 11, the number of stations is fixed to 25 as well as the duration to medium ($T_{if} = 50$). The effect of the probability can be seen especially in the simulation where the difference to the measurements ranges from 6% to 27% while the simulation maintains a difference of 9% and is much more reliable.

Our model performs well in predicting the throughput and, contrary to simulation, can give an accurate value for each scenario that we explored. Our model also performs better than state-of-the-art models like the one from Pham [9] or Chella et al. [21] that do not include external interference [9,21].

5.4. Asymptotic analysis

In this section, we evaluate the average packet delay in case of low load (i.e. λ small) and in case of high load (i.e., for high values of λ). In case of low load, we assume that the packet queue is empty upon arrival of a packet. Hence, the average delay, in that case, is given by the average service time a packet experiences, given by

$$E[V] = \sum_{i=0}^{m+1} E[A]_i \cdot \frac{p^i \cdot (1-p)}{1-p^{m+2}} \tag{54}$$

In case of a high load, we assume that a tagged packet arrives at a queue with $Q_l - 1$ packets. Those $Q_l - 1$ packets are served before the tagged packet. The service of a packet may be a successful transmission or the dropping of a packet. Hence, the service time of each of these $Q_l - 1$ packets is given by

$$E[S] = \sum_{i=0}^{m+1} E[A]_i \cdot p^i \cdot (1-p) + E[A]_{m+2} \cdot (1-p^{m+2}) \tag{55}$$

The average delay of the tagged packet is then given by the sum of the service times $E[S]$ of the $Q_l - 1$ packets and the service time of the tagged packet

$$E[V] = (Q_l - 1) \cdot E[S] + \sum_{i=0}^{m+1} E[A]_i \cdot \frac{p^i \cdot (1-p)}{1-p^{m+2}} \tag{56}$$

In what follows, we apply this asymptotic analysis to the following example. Let $T_{if} = 50$, $p_{if} = 0.01$ and let the number of stations vary $n = 5, 10, 15, 20, 25$. We compute for each n the values of p and τ under low load, i.e., $\lambda = 5$, and under high load, i.e., $\lambda = 400$. These values of p

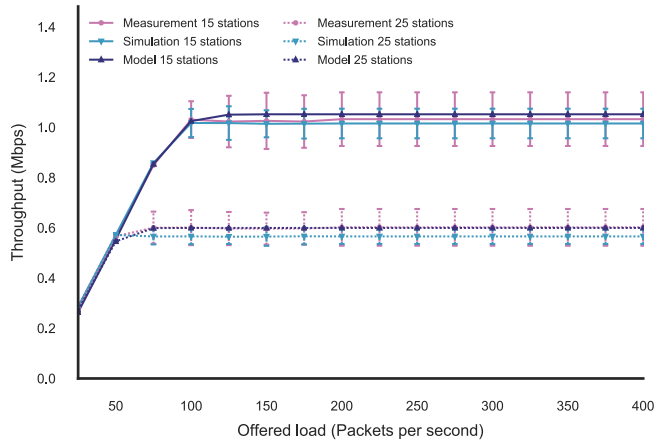

(a) Low interference occurrence and medium duration.

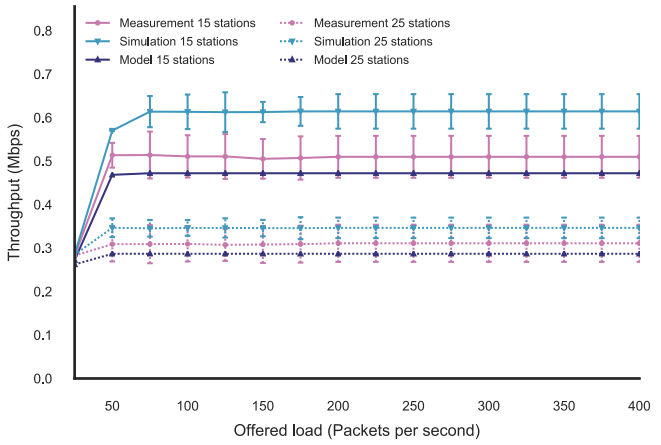

(b) High interference occurrence and medium duration.

Fig. 9. Throughput for fixed interference occurrence, fixed medium duration, and changing number of stations.

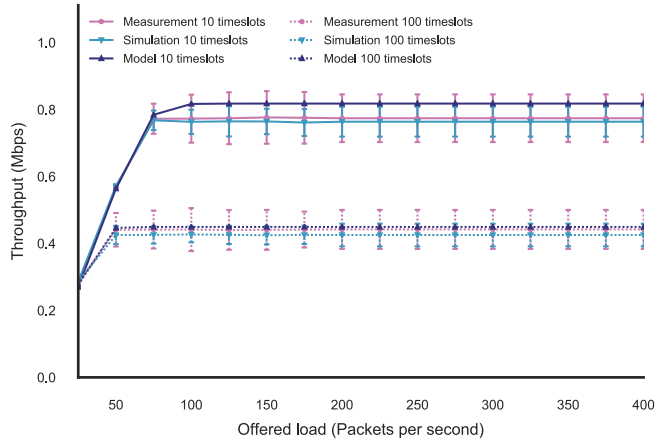

(a) Low interference occurrence and 25 stations.

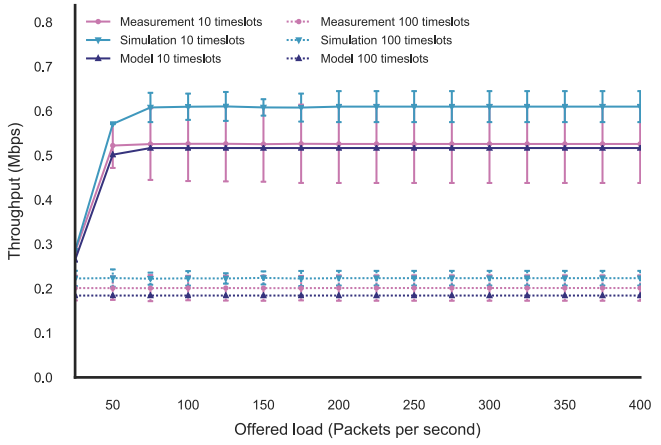

(b) High interference occurrence and 25 stations.

Fig. 10. Throughput for fixed interference occurrence, fixed number of stations, and changing duration.

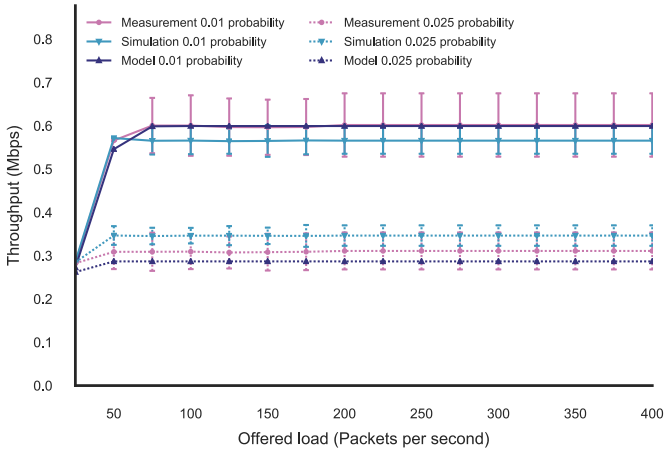

Fig. 11. Throughput for medium duration, 25 stations, and changing occurrence.

and τ allow to compute the average delay making use of the above formulas. In Fig. 12, for each value of n, the average delay for variable λ is shown using the detailed model, together with the low and high load asymptotic. We can see that the asymptotes fit in the low load scenario, as well as the high load scenario.

5.5. Parameter exploration

In this section, we will explore the influence of the parameters p_{if}, T_{if}, and ω, as well as the impact of the RTS/CTS mechanism on the latency and throughput.

5.5.1. RTS/CTS mechanism

The RTS/CTS mechanism has the goal of reducing collisions, especially for hidden terminals. Fig. 13a and b show a low and high load scenario, respectively, for latency based on an increasing client number. Model and simulation show a higher latency with RTS/CTS enabled. The throughput using the basic mechanism and using the RTS/CTS scheme are very close to each other as shown in Fig. 14a and b. While the throughput remains close to the basic mechanism with an increasing

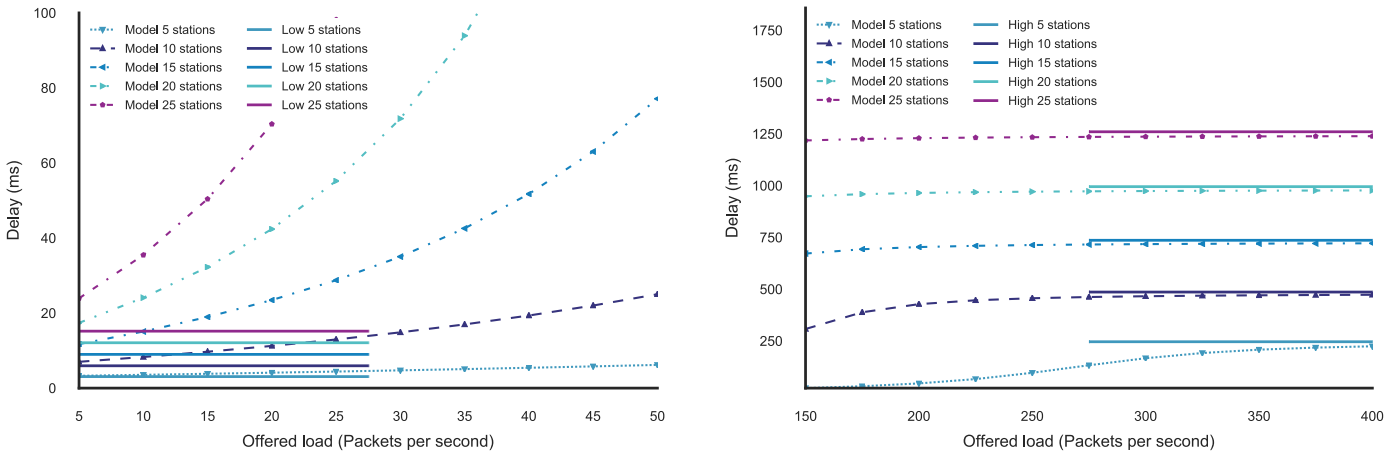

(a) Low asymptote. (b) High asymptote.

Fig. 12. Latency for fixed interference and different number of stations with asymptotes for high and low load.

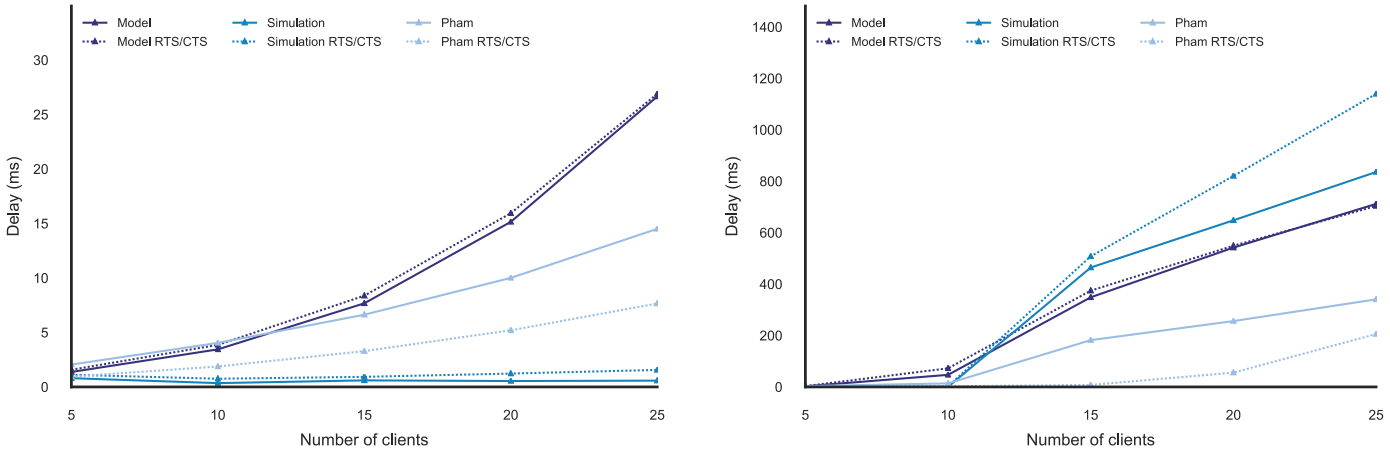

(a) Low load. (b) High load.

Fig. 13. Latency comparison of RTS/CTS mechanism to basic mechanism with simulation, based on clients.

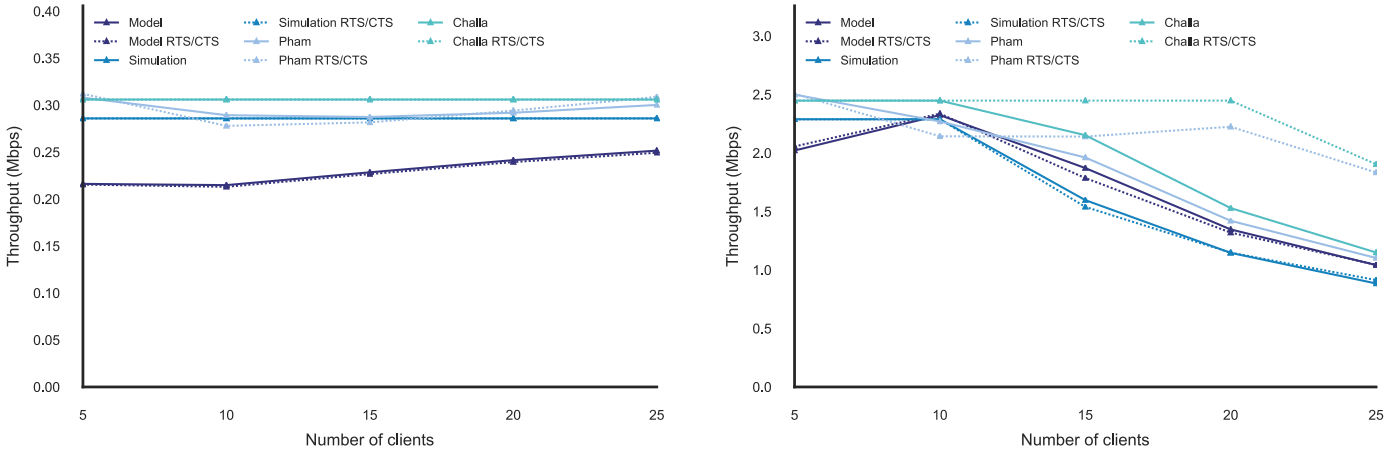

(a) Low load. (b) High load.

Fig. 14. Throughput comparison of RTS/CTS mechanism to basic mechanism with simulation, based on clients.

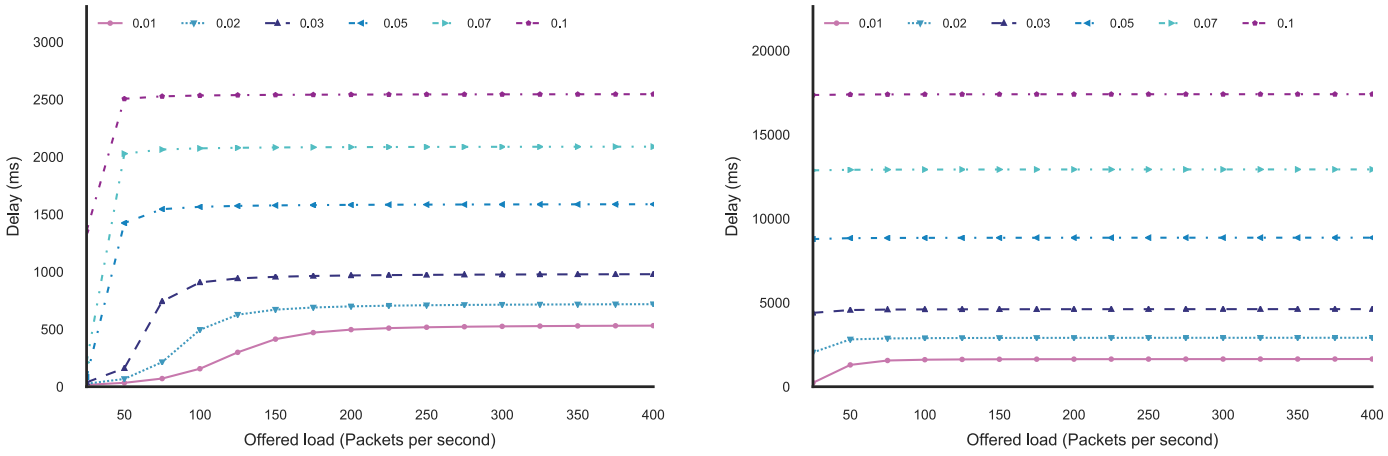

(a) 15 stations and low duration. (b) 25 stations and high duration.

Fig. 15. Latency comparison of model with varying occurrence and fixed number of stations and duration.

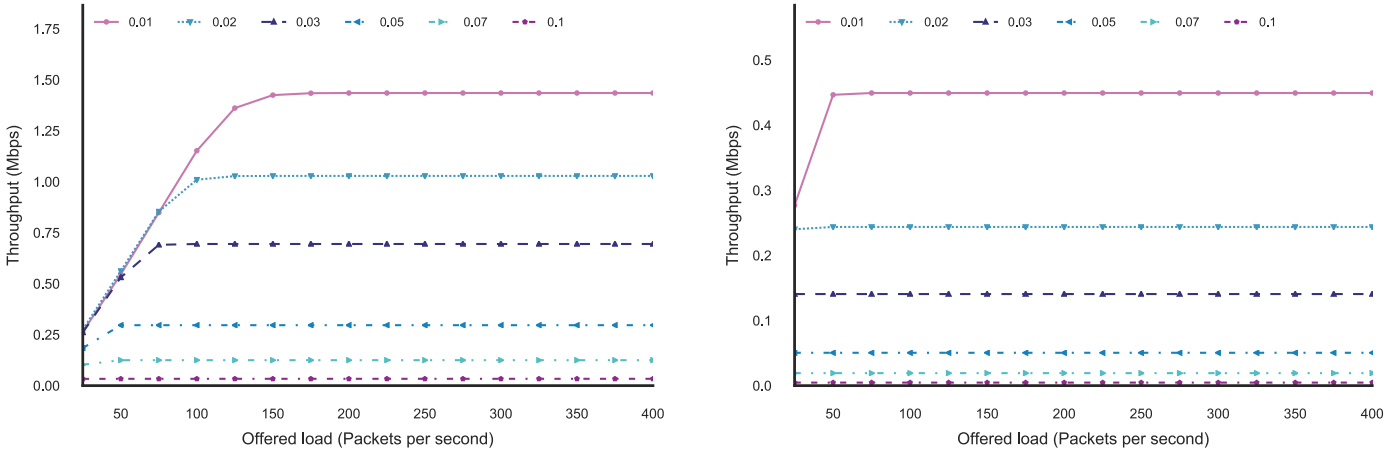

(a) 15 stations and low duration. (b) 25 stations and high duration.

Fig. 16. Throughput comparison of model with varying occurrence and fixed number of stations and duration.

number of stations, the latency further increases in that case. The improvement that the RTS/CTS mechanism shows in low bandwidth scenarios with DSSS and the reduction of T_c seems negated by the use of higher bandwidth and OFDM as the encoding scheme.

From a performance viewpoint, the RTS/CTS mechanism does not have a strong impact on higher bandwidths. The difference to the basic mechanism is minimal and therefore it can not always be recommended.

5.5.2. Interference occurrence

Figs. 15 and 16 show the latency and throughput for a variety of values for p_{if} with a fixed number of stations and duration. In both cases, a low number of stations and low duration, as well as a high number of stations and high duration, an increase of p_{if} is combined with a significant increase in latency. In the first case, the increase is roughly five times the lowest value of p_{if} to the highest. In the second case, that increase is around ten times. Both the increase in duration and number of stations add to the problem that a high interference occurrence is causing. Similar to latency, the throughput also drops significantly, but much more than latency. In the case of a low number of stations and low duration, it loses 97.5% of throughput from the lowest value of p_{if} to the highest. With a high number of stations and high duration, it loses even up to 99% of its throughput.

We can conclude that the increase in interference occurrence has a much higher impact on throughput than latency.

5.5.3. Interference duration

Similar to the interference occurrence, we also explore the duration in Figs. 17 and 18. With increased duration, latency increases by a bit less than three times for a low number of stations and low occurrence and up to six times for a high number of stations and a high occurrence. It is interesting to note, though, that an up to 20 times increase of duration has much less impact than a ten times increase of occurrence. The decrease in throughput scales like the increase in latency, and we have up to three times and six times reduction in throughput from the lowest value for T_{if} up to the highest.

We can conclude that while duration has an impact, it has a significantly smaller impact than occurrence. This difference in impact has to do with the ED function of IEEE 802.11, where a higher occurrence has a higher probability of triggering an additional back-off phase.

5.5.4. FEC mechanism

In Figs. 19 and 20, we can see the effect of ω, the probability that the FEC mechanism can recover the packet, although it had a collision with the interfering source, on the latency and throughput. The latency

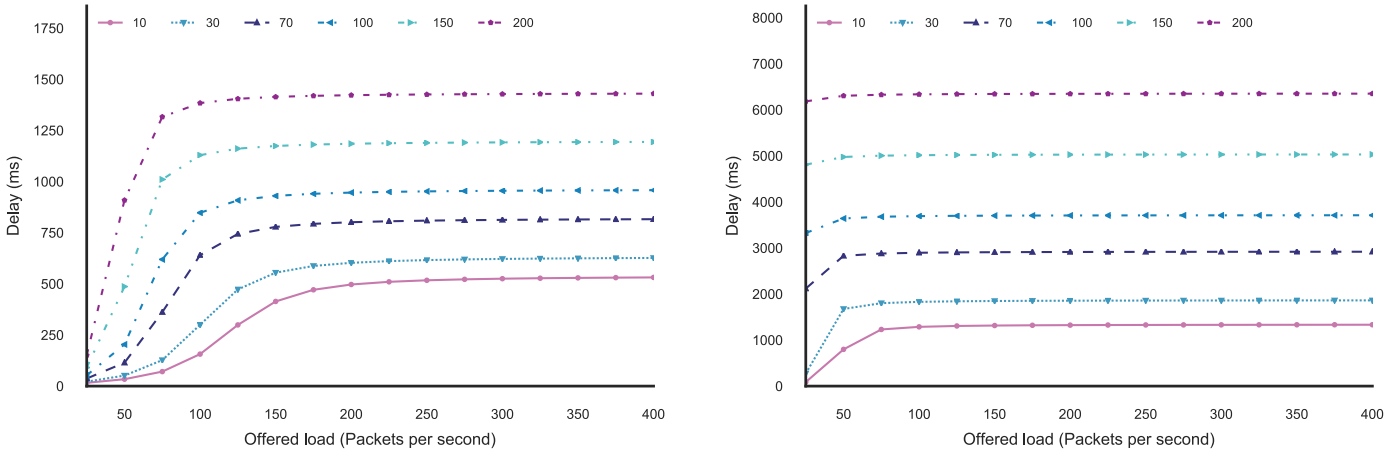

(a) 15 stations and low occurrence. (b) 25 stations and high occurrence.

Fig. 17. Latency comparison of model with varying duration and fixed number of stations and occurrence.

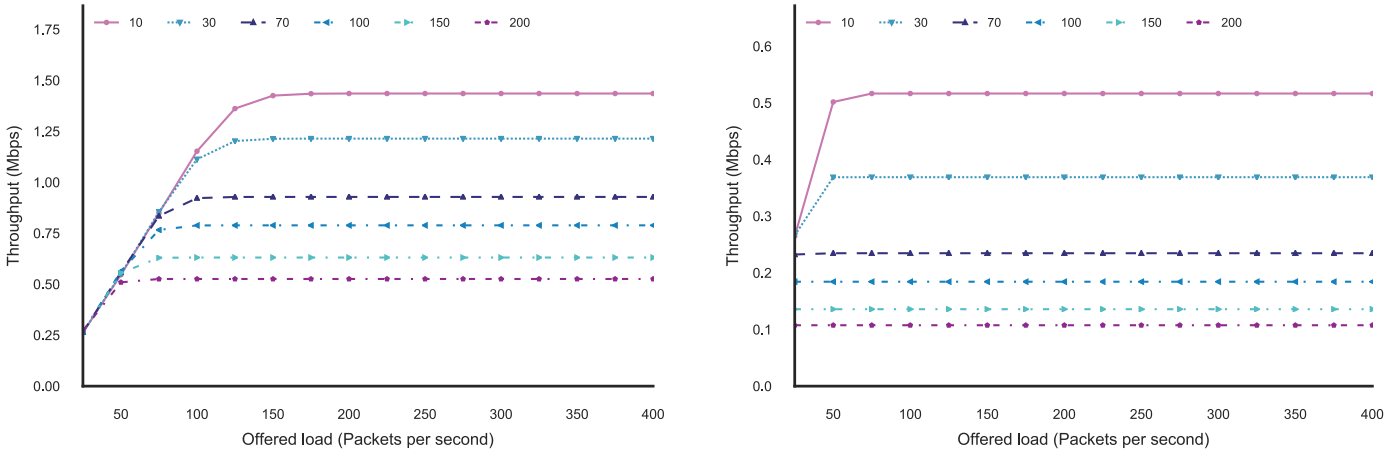

(a) 15 stations and low occurrence. (b) 25 stations and high occurrence.

Fig. 18. Throughput comparison of model with varying duration and fixed number of stations and occurrence.

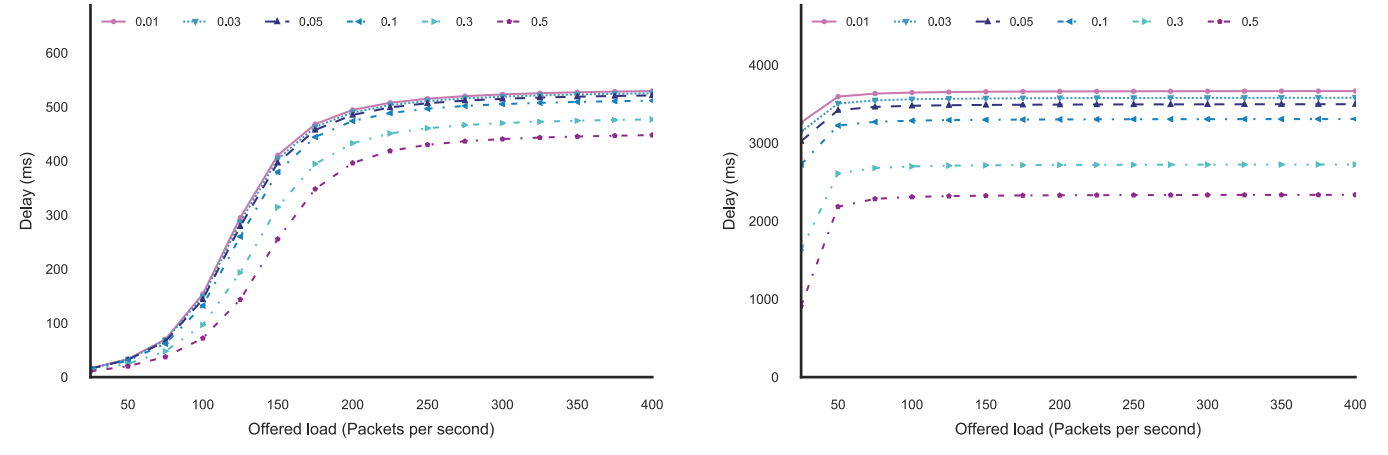

(a) 15 stations, low occurrence, and low duration. (b) 25 stations, high occurrence, and high duration.

Fig. 19. Latency comparison of model with varying ω and fixed duration, number of stations, and occurrence.

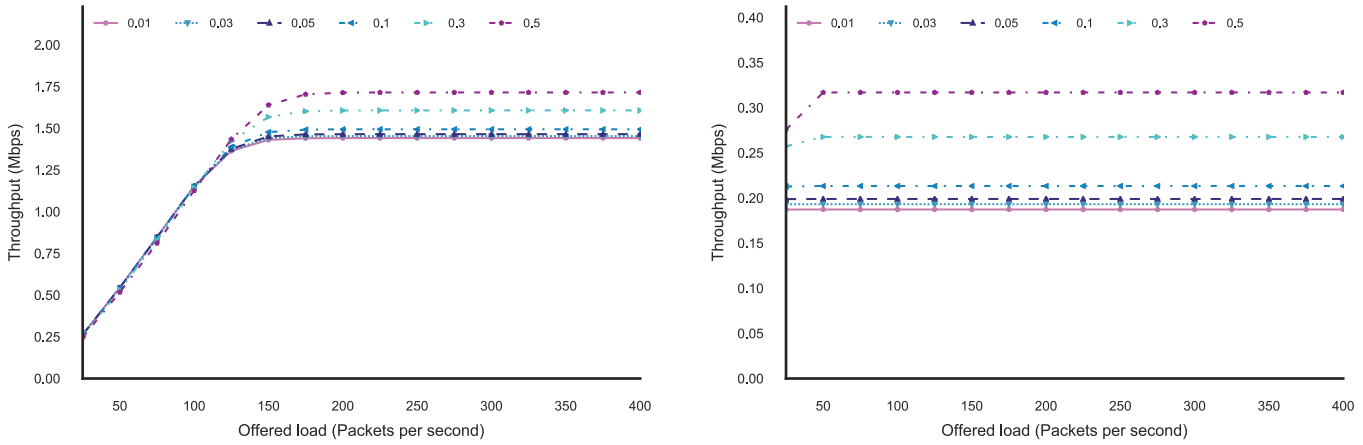

(a) 15 stations, low occurrence, and low duration.

(b) 25 stations, high occurrence, and high duration.

Fig. 20. Latency comparison of model with varying ω and fixed duration, number of stations, and occurrence.

reduction reaches from 0.4% for $\omega = 0.01$ to 16% for $\omega = 0.5$ in the case of a low number of stations, low occurrence, and low duration. With a high number of stations, high occurrence, and high duration, the reduction reaches from 1.3% for $\omega = 0.01$ to 37% for $\omega = 0.5$. In both cases, the reduction scales slightly lower than linear with the value of ω.

If we look at the throughput in Fig. 20, we can see that an even more significant improvement is achieved. In the first case, the increase reaches from 0.7% to 19.5%, and in the second case, from 1.6% to 72%. While in the first case, it does scale lower than linear, in the second case, it scales significantly better than linear.

We can conclude that the FEC mechanism can have a significant impact on latency and throughput with high interference. For high interfering cases, an improvement of the FEC mechanism is worthwhile.

6. Conclusions

In this paper, we presented an analytical model to predict latency and throughput in an IEEE 802.11 system with non-IEEE 802.11 interfering source based on a Markov chain to model the back-off mechanism. We cover both, saturated as well as unsaturated network conditions by utilizing a QBD process as the model for the packet queue of a station. The interfering source is accurately described to be included in the model. The results show that our model is in most cases within 10% difference between the model and measurements, for both, latency and throughput, while the simulation is not. These values show that we can accurately model an interfering source and describe the impact it has on performance, which can be used in network management.

Declaration of Competing Interest

The authors declare that they have no known competing financial interests or personal relationships that could have appeared to influence the work reported in this paper.

CRediT authorship contribution statement

Patrick Bosch: Conceptualization, Methodology, Software, Validation, Formal analysis, Investigation, Data curation, Writing - original draft, Writing - review & editing, Visualization, Project administration, Funding acquisition. **Steven Latré:** Conceptualization, Resources, Writing - review & editing, Supervision, Funding acquisition. **Chris Blondia:** Conceptualization, Methodology, Writing - review & editing, Supervision.

Acknowledgment

Patrick Bosch is funded by FWO, a fund for fundamental scientific research, and the Flemish Government, under grant number 1S56616N. The authors would like to thanks the reviewers for the valuable remarks and suggestions.

References

[1] G. Bianchi, IEEE 802.11-Saturation throughput analysis, IEEE Commun. Lett. 2 (12) (1998) 318–320, doi:10.1109/4234.736171.
[2] P. Bosch, J. Wyffels, B. Braem, S. Latre, How is your event Wi-Fi doing? Performance measurements of large-scale and dense IEEE 802.11n/ac networks, in: 2017 IFIP/IEEE Symposium on Integrated Network and Service Management (IM), 2017, pp. 701–707, doi:10.23919/INM.2017.7987362. Im.
[3] P. Bosch, S. Latre, C. Blondia, Latency Modelling in IEEE 802.11 Systems with non-IEEE 802.11 Interfering Source, in: 2018 14th International Conference on Network and Service Management (CNSM), 2018, pp. 275–279.
[4] A.M. Cavalcante, E. Almeida, R.D. Vieira, S. Choudhury, E. Tuomaala, K. Doppler, F. Chaves, R.C.D. Paiva, F. Abinader, Performance Evaluation of LTE and Wi-Fi Coexistence in Unlicensed Bands, in: 2013 IEEE 77th Vehicular Technology Conference (VTC Spring), 2013, pp. 1–6, doi:10.1109/VTCSpring.2013.6692702. April 2015.
[5] S. Sagari, I. Seskar, D. Raychaudhuri, Modeling the coexistence of LTE and WiFi heterogeneous networks in dense deployment scenarios, in: 2015 IEEE International Conference on Communication Workshop (ICCW), 2015, pp. 2301–2306, doi:10.1109/ICCW.2015.7247524.
[6] I. Gomez-Miguelez, A. Garcia-Saavedra, P.D. Sutton, P. Serrano, C. Cano, D.J. Leith, srsLTE: an open-source platform for LTE evolution and experimentation, in: Proceedings of the Annual International Conference on Mobile Computing and Networking, MOBICOM, 03–07–Octo, 2016, pp. 25–32, doi:10.1145/2980159.2980163.
[7] C. Capretti, F. Gringoli, N. Facchi, P. Patras, LTE/Wi-Fi co-existence under scrutiny: an empirical study, in: Proceedings of the Annual International Conference on Mobile Computing and Networking, MOBICOM, 03–07–Octo, 2016, pp. 33–40, doi:10.1145/2980159.2980164.
[8] IEEE Computer Society, IEEE Standard for information technology–telecommunications and information exchange between systems local and metropolitan area networks–Specific requirements - Part 11: wireless LAN medium access control (MAC) and physical layer (PHY) specifications, IEEE Std 802.11–2016 (Revision of IEEE Std 802.11–2012) 2016 (2016) 1–3534, doi:10.1109/IEEESTD.2016.7786995.
[9] P.P. Pham, Comprehensive analysis of the IEEE 802.11, Mob. Netw. Appl. 10 (5) (2005) 691–703, doi:10.1007/s11036-005-3363-x.
[10] G. Bianchi, Performance analysis of the IEEE 802.11 distributed coordination function, IEEE J. Sel. Areas Commun. 18 (3) (2000) 535–547, doi:10.1109/49.840210.
[11] Haitao Wu, Yong Peng, Keping Long, Shiduan Cheng, Jian Ma, H. Wu, Y. Peng, K. Long, S. Cheng, J. Ma, Performance of reliable transport protocol over IEEE 802.11 wireless LAN: analysis and enhancement, in: Proceedings - IEEE INFOCOM, 2, 2002, pp. 599–607, doi:10.1109/INFCOM.2002.1019305.
[12] P. Chatzimisios, A. Boucouvalas, V. Vitsas, IEEE 802.11 packet delay - a finite retry limit analysis, in: GLOBECOM '03. IEEE Global Telecommunications Conference (IEEE Cat. No.03CH37489), 2, 2003a, pp. 950–954, doi:10.1109/GLOCOM.2003.1258379.

[13] P. Chatzimisios, A. Boucouvalas, V. Vitsas, Influence of channel BER on IEEE 802.11 DCF, Electron. Lett. 39 (23) (2003b) 1687, doi:10.1049/el:20031081.
[14] I. Vukovic, N. Smavatkul, Delay analysis of different backoff algorithms in IEEE 802.11, in: IEEE 60th Vehicular Technology Conference, 2004. VTC2004-Fall. 2004, 6, 2004, pp. 4553–4557, doi:10.1109/VETECF.2004.1404941.
[15] P. Chatzimisios, A.C. Boucouvalas, V. Vitsas, Performance analysis of the IEEE 802.11 MAC protocol for wireless LANs, Int. J. Commun. Syst. 18 (6) (2005) 545–569, doi:10.1002/dac.717.
[16] T. Sakurai, H.L. Vu, MAC Access delay of IEEE 802.11 DCF, IEEE Trans. Wireless Commun. 6 (5) (2007) 1702–1710, doi:10.1109/TWC.2007.360372.
[17] Y. Li, C. Wang, K. Long, W. Zhao, Modeling channel access delay and jitter of IEEE 802.11 DCF, Wireless Pers. Commun. 47 (3) (2008) 417–440, doi:10.1007/s11277-008-9491-4.
[18] P. Raptis, V. Vitsas, K. Paparrizos, Packet delay metrics for IEEE 802.11 distributed coordination function, Mob. Netw. Appl. 14 (6) (2009) 772–781, doi:10.1007/s11036-008-0124-7.
[19] N. Lei, T. Zhang, L. Zhou, X. Song, S. Cai, Saturation throughput analysis of IEEE 802.11 DCF with heterogeneous node transmit powers and capture effect, Int. J. Ad Hoc Ubiquitous Comput. 26 (1) (2017) 1, doi:10.1504/IJAHUC.2017.085716.
[20] O. Tickoo, O. Sikdar, Modeling queueing and channel access delay in unsaturated IEEE 802.11 random access MAC based wireless networks, IEEE/ACM Trans. Networking 16 (4) (2008) 878–891, doi:10.1109/TNET.2007.904010.
[21] R.K. Challa, S. Chakrabarti, D. Datta, An improved analytical model for IEEE 802.11 distributed coordination function under finite load, Int. J. Commun. Netw. Syst. Sci. 2 (3) (2009) 237–247, doi:10.4236/ijcns.2009.23026.
[22] F. Daneshgaran, M. Laddomada, F. Mesiti, M. Mondin, Unsaturated throughput analysis of IEEE 802.11 in presence of non ideal transmission channel and capture effects, IEEE Trans. Wireless Commun. 7 (4) (2008) 1276–1286, doi:10.1109/TWC.2008.060859.
[23] A.M. Abbas, K.A.M.A. Soufy, A queue state driven analysis of IEEE 802.11 DCF for ad hoc networks under non-saturation conditions, Int. J. Comput. Sci. Eng. 12 (2/3) (2016) 237, doi:10.1504/IJCSE.2016.076214.
[24] E. Felemban, E. Ekici, Single hop IEEE 802.11 DCF analysis revisited: accurate modeling of channel access delay and throughput for saturated and unsaturated traffic cases, IEEE Trans. Wireless Commun. 10 (10) (2011) 3256–3266, doi:10.1109/TWC.2011.072511.101227.
[25] G. Tian, Y.C. Tian, Markov modelling of the IEEE 802.11 DCF for real-time applications with periodic traffic, in: Proceedings - 2010 12th IEEE International Conference on High Performance Computing and Communications, HPCC 2010, 2010, pp. 419–426, doi:10.1109/HPCC.2010.51. September.
[26] C. Xu, K. Liu, G. Liu, J. He, Accurate Queuing Analysis of IEEE 802.11 MAC Layer, in: IEEE GLOBECOM 2008 - 2008 IEEE Global Telecommunications Conference, 2008, pp. 1–5, doi:10.1109/GLOCOM.2008.ECP.66. ii.
[27] Y.W. Kuo, W.F. Lu, T.L. Tsai, A framework to approximate the delay distribution for IEEE 802.11 DCF protocol, in: Proceedings - MICC 2009: 2009 IEEE 9th Malaysia International Conference on Communications with a Special Workshop on Digital TV Contents, 2009, pp. 874–879, doi:10.1109/MICC.2009.5431454. December.
[28] L. Xie, H. Wang, G. Wei, Z. Xie, Performance analysis of IEEE 802.11 DCF in multi-hop ad hoc networks, in: 2009 International Conference on Networks Security, Wireless Communications and Trusted Computing, 2009, pp. 227–230, doi:10.1109/NSWCTC.2009.84.
[29] M. Mehrnoush, V. Sathya, S. Roy, M. Ghosh, Analytical modeling of wi-Fi and LTE-LAA coexistence: throughput and impact of energy detection threshold, IEEE/ACM Trans. Networking 26 (4) (2018) 1990–2003, doi:10.1109/TNET.2018.2856901.
[30] S. Gollakota, F. Adib, D. Katabi, S. Seshan, Clearing the RF smog: Making 802.11 Robust to Cross-Technology Interference, in: Proceedings of the ACM SIGCOMM 2011 conference on SIGCOMM - SIGCOMM '11, 41, 2011, p. 170, doi:10.1145/2018436.2018456.
[31] A. Hithnawi, H. Shafagh, S. Duquennoy, Understanding the impact of cross technology interference on IEEE 802.15.4, in: Proceedings of the 9th ACM international workshop on Wireless network testbeds, experimental evaluation and characterization - WiNTECH '14, 2014, pp. 49–56, doi:10.1145/2643230.2643235.
[32] R. Gummadi, D. Wetherall, B. Greenstein, S. Seshan, Understanding and mitigating the impact of RF interference on 802.11 networks, in: Proceedings of the 2007 conference on Applications, technologies, architectures, and protocols for computer communications - SIGCOMM '07, 2007, p. 385, doi:10.1145/1282380.1282424.
[33] A. Conti, D. Dardari, G. Pasolini, O. Andrisano, Bluetooth and IEEE 802.11b coexistence: analytical performance evaluation in fading channels, IEEE J. Sel. Areas Commun. 21 (2) (2003) 259–269, doi:10.1109/JSAC.2002.807345.
[34] Jung-Hyuck Jo, H. Jayant, Performance evaluation of multiple IEEE 802.11b WLAN stations in the presence of Bluetooth radio interference, in: IEEE International Conference on Communications, 2003. ICC '03., 2, 2003, pp. 1163–1168, doi:10.1109/ICC.2003.1204550.
[35] K. Shuaib, M. Boulmalf, F. Sallabi, A. Lakas, Co-existence of Zigbee and WLAN, A Performance Study, in: 2006 Wireless Telecommunications Symposium, 2006, pp. 1–6, doi:10.1109/WTS.2006.334532.
[36] H. Huo, Y. Xu, C.C. Bilen, H. Zhang, Coexistence Issues of 2.4GHz Sensor Networks with Other RF Devices at Home, in: 2009 Third International Conference on Sensor Technologies and Applications, 2009, pp. 200–205, doi:10.1109/SENSORCOMM.2009.40.
[37] K. Bicakci, B. Tavli, Denial-of-Service attacks and countermeasures in IEEE 802.11 wireless networks, Computer Standards & Interfaces 31 (5) (2009) 931–941, doi:10.1016/j.csi.2008.09.038.
[38] V. de Nitto Personé, V. Grassi, Solution of finite QBD processes, J Appl Probab 33 (4) (1996) 1003–1010, doi:10.2307/3214981.
[39] S.K. Gupta, J.K. Goyal, Queues with poisson input and hyper-Exponential output with finite waiting space, Oper Res 12 (1) (1964) 75–81, doi:10.1287/opre.12.1.75.

Patrick Bosch is a Ph.D. researcher associated with imec and the University of Antwerp, Belgium. He received his Diploma degree in Computer Science from the University of Stuttgart, Germany in 2014. His Diploma thesis centered around optimizing content routing in an SDN based publish/subscribe system. His current research focuses on network orchestration and management of different wireless technologies to improve Quality of Service, interference modeling for wireless networks, and network management. His research resulted in 8 articles published in international peer-reviewed journals and conference proceedings, as well as in two submitted patent applications.

Prof. Steven Latré is an associate professor at the University of Antwerp and director at the research center imec, Belgium. He is leading the IDLab Antwerp research group (85+ members), which is performing applied and fundamental research in the area of communication networks and distributed intelligence. His personal research interests are in the domain of machine learning and its application to wireless network optimization. He received a Master of Science degree in computer science from Ghent University, Belgium and a Ph.D. in Computer Science Engineering from the same university with the title "Autonomic Quality of Experience Management of Multimedia Services." He is author or co-author of more than 100 papers published in international journals or the proceedings of international conferences. He is the recipient of the IEEE COMSOC award for best Ph.D. in network and service management 2012, the IEEE NOMS Young Professional award 2014 and is a member of the Young Academy Belgium.

Chris Blondia obtained his Master in Science and Ph.D. in Mathematics, both from the University of Ghent (Belgium) in 1977 and 1982 respectively. In 1983 he joined Philips Belgium, where he was a researcher between 1986 and 1991 in the Philips Research Laboratory Belgium (PRLB) in the group Computer and Communication Systems. Between August 1991 and end 1994 he was an Associate Professor in the Computer Science Department of the University of Nijmegen (The Netherlands). In 1995 he joined the Department of Mathematics and Computer Science of the University of Antwerp, where he is currently a Full Professor in the Internet and Data Lab (IDLab) research group. He has been the Chair of the Department of Mathematics and Computer Science between 2010 and 2016. He is lecturing networking courses. His main research interests are related to the design, analysis, and implementation of algorithms and protocols for communication networks, in particular, wireless networks, focusing on their performance. He has published over 250 papers in international journals and conferences on these research areas. He has been involved in many national and European Research Programs. The IDLab research group is also a core group of the Flemish Strategic Research Center imec (www.imec.be).